RECHARGE AND BASEFLOW OF A FIRST ORDER STREAM IN THE PIEDMONT

by

BRIAN MATTHEW PRICE

(Under the Direction of JOHN F. DOWD)

ABSTRACT

A groundwater model is applied to a rural watershed to evaluate the impact of urbanization on groundwater recharge and baseflow. The saturated zone model of a zero order watershed near Watkinsville, Georgia, an area of the Piedmont physiographic region, was developed to simulate 423 days of hydraulic data. A sensitivity analysis was performed to evaluate uncertainties in model parameters. Five land use scenarios were investigated: (1) A rural pasture; a housing development on (2) city sewer; (3) with leaky sewer/water lines; (4) with septic sewer; and (5) with septic sewer and single home wells. While the methodology is useful in predicting baseflow differences between land uses, the results are sensitive to yearly climatic conditions reflected in the initial conditions.

INDEX WORDS: Urbanization, Groundwater recharge, Numerical model, Saturated zone, Finite element method, Piedmont

RECHARGE AND BASEFLOW OF A FIRST ORDER STREAM IN THE PIEDMONT

by

BRIAN MATTHEW PRICE

B.S., University of Georgia, 2006

A Thesis Submitted to the Graduate Faculty of The University of Georgia in Partial Fulfillment of the Requirements for the Degree

MASTER OF SCIENCE

ATHENS, GEORGIA

2010

RECHARGE AND BASEFLOW OF A FIRST ORDER STREAM IN THE PIEDMONT

by

BRIAN MATTHEW PRICE

Major Professor:	John F. Dowd
Committee:	Dinku Endale Christof Meile Todd Rasmussen

Electronic Version Approved:

Maureen Grasso
Dean of the Graduate School
The University of Georgia
August 2010

DEDICATION

I dedicate this to: 1) My family who helped me through school, 2) My committee for helping me complete my MS, 3) My friends who are always good for more than a few laughs, 4) My wife Ellen.

ACKNOWLEDGEMENTS

I would like to acknowledge first and foremost my advisor John Dowd for his insight and critical thinking. I would like to acknowledge my committee members Dinku Endale of the USDA-ARS, Todd Rasmussen, and Christof Meile who provided very insightful comments and constructive criticism. I would like to thank Stephen Norris at the USDA-ARS for going out of his way to help me with my field work; and thank all my professors and instructors. These people have contributed to my training to some capacity, and, without a doubt, this work would never have been completed without them.

I would also like to acknowledge the USDA-ARS, J. Phil Campbell Sr. Natural Resource Conservation Center for allowing access to the site, allowing use of existing hydrologic infrastructure (wells and flumes), allowing use of existing monitoring equipment, and for providing flow records for use in calibration and validation, rainfall records, spring flow records, and barometric pressure records.

TABLE OF CONTENTS

Page

LIST OF TABLES

Page

LIST OF FIGURES

Page

Chapter 1: Introduction

The southeastern United States is experiencing rapid population growth. Georgia's population has increased 18.3% from April 2000 to July 2008 (2010). The increase in population has increased urbanization and the use of the natural resources in Georgia, particularly fresh water.

Currently, much of the Piedmont relies on surface water as its source of water because of its proximity to the headwaters of several large rivers and because finding suitable high yielding wells is difficult. In Atlanta alone, surface water supplies more than 98.5 % of the water used because the underlying aquifer does not typically support high yield wells (Fanning, 2003). However, as a result of the water feud between Georgia, Alabama, and Florida, the city of Atlanta is in danger of being restricted from using water from Lake Lanier as municipal water source by 2012 (Rankin, 2009).

The influence of urbanization on groundwater recharge is unclear. Recharge is defined as, "…entry into the saturated zone of water made available at the watertable surface together with the associated flow away from the water table within the saturated zone." (Freeze and Cherry, 1979). McCuen (2005) states that urbanization, with the accompanying loss of vegetation, replacement of soil with impervious surfaces, and storm-flow routing to stream channels has a substantial impact on many of the processes that control streamflow. Shaw (1994) identifies five major effects of urbanization: (1) Increased surface runoff; (2) decreased lag time (the time difference between the centroid of the storm and the peak of the hydrograph); (3) increased peak flow magnitudes for all storms except the largest; (4) degraded water quality

due to effluent discharge; and (5) reduced low flow in streams. A streamflow comparison study by Rose and Peters (2001) in the Atlanta area concludes that low flows in an urbanized stream have declined relative to a non-urbanized stream since urbanization has increased and that water levels in an urban well have decreased relative to water levels measured in a rural well. They state that reduced low flows and water levels in wells can be attributed to the increase in percent impervious surface in the urbanized area.

Lerner (2002) makes a contrary argument. He divides the sources of recharge in urban areas into three groups: (1) Direct recharge that occurs from precipitation, (2) Indirect recharge that occurs from leaky water, sewer mains, and other man made features, and (3) Localized recharge that occurs at sinkholes and open bore holes. He states that although urbanization increases percent impervious surface and decreases direct recharge, leaky utilities introduce new pathways for water to recharge groundwater which compensates for the decrease in direct recharge. He cites several studies that agree with this claim: Brassington and Rushton (1987); Foster (1988); Lerner (1986); and Price and Reed (1989).

Landers *et al.* (2007) state that there is a critical threshold for the percentage of impervious area in a watershed that must be exceeded before hydrologic impacts can be observed. The location of the impervious area in relation to water body factors into the threshold, but hydrologic impact can be observed when percent impervious surface reaches 12% in most watersheds.

1.1 Objectives of the Study

From a water resource planning perspective, it is desirable to evaluate the outcome of the worst case scenario. In this case, the worst case scenario is reduced direct recharge due to urbanization without any compensation for the decrease in recharge by leaky utilities. This work

presents a method to evaluate the worst case scenario. This methodology is also useful as a tool to evaluate whether or not utilities are leaking significant amounts of water in times of water shortages.

The other objectives of this study are: (1) Formulate a conceptual and mathematical description of two dimensional, planimetric (x,y), groundwater flow in heterogeneous media under non steady-state conditions in the Georgia Piedmont. (2) Develop a model domain with Comsol Multiphysics, a commercial finite element analysis, simulation, and visualization tool. This includes developing the groundwater model domain and using Comsol's automatic mesh generator. (3) Calibrate the mathematical expression in Comsol by adjusting recharge rates and hydraulic conductivity to match head observations in wells at the field site thus resulting in a calibrated steady state solution of the watertable; and then, (4) use the steady-state solution as the initial conditions for a 423 day simulation of the watertable dynamics and groundwater discharge to the wetland using Comsol in five scenarios: A rural scenario (the field sites current land use), an urban scenario (with a housing development without any leaky water utilities), a leaky urban scenario (with a housing development with leaky water and sewer lines), a septic scenario (with a housing development with septic tanks that provide recharge), and a septic well scenario (with a housing development with septic tanks that provide recharge and single home wells that withdraw water from the aquifer).

1.2 Modeling Approach (Method of Solution)

One form of intensive hydrologic investigation is the development, calibration, and application of a numerical simulation model. The use of a numerical simulation model tends to lead to an increased understanding of the system under investigation faster than could be achieved only using a conceptual model. The application of the model to investigation of

groundwater contributions to surface water is achieved by the use of predictive, two-dimensional in planar orientation, finite element model that simulates groundwater flow in heterogeneous media under transient conditions. In general, the initial steps require the development of a conceptual model of the groundwater system. This entails the identification of essential geologic formations and major hydrostratigraphic units in which the watertable is located. Water bodies are located and watertable contour maps are used to delineate flow lines. Head data are collected for some time. A finite element model is developed and calibration is performed by adjusting recharge rates and hydraulic conductivity so that calculated heads are acceptably close to observed heads. Uncertainties incorporated in the calibration process are evaluated by performing a series of sensitivity tests in which the system response is inspected as each hydrologic factor is changed regularly and individually.

Flux across the constant head boundary is then calculated by numerically integrating around the constant head boundaries and total outward normal flux is calculated for 423 days, which was the duration of the simulation. Runoff is estimated for 1yr-24hr, 2yr-24hr, 5yr-24hr, 10yr-24hr, 25yr-24hr, 50yr-24hr, and 100yr-24hr storms using the curve number (Cronshey, 1975) for the site's current land use and for the site's proposed land use. Calibrated recharge is reduced by subtracting the average difference in runoff divided by the number of days that model calibrated recharge is not zero from the transient model calibrated recharge rate. Flux across the constant head boundaries are calculated again using the reduced recharge rate for the duration of the simulation. See Figure 1 for a flow chart of the solution method.

1.3 Limitations of the Study

In the Piedmont of Georgia (see Figure 2), the major groundwater resource is the saprolite and fractured bedrock stratigraphic units that comprise one aquifer (LeGrand, 1989)

Because it is impractical to survey all aquifers, this study will only examine those conditions that can reasonably be inferred for Watershed 2 (see the field site maps in Figure 3 and Figure 4) near Watkinsville, Georgia. This limits the study to an examination of flow in unconsolidated saprolite which is assumed to have uniform physical properties. The study assumes the potential for flow through fractures in the crystalline bedrock that underlies the saprolite is negligible.

The methodology described in chapter four employs the Soil Conservation Service Curve Number method outlined in TR-55 (Cronshey, 1975) and the Natural Resource Conservation Center's winTR-20 (S.C.S, 1965) program, and, therefore, the limits of the curve number extend to the methodology employed in this work. The methodology used for predicting the amount of recharge that occurs in an urbanized setting can only be considered a first approximation of the actual recharge rate in any housing development. This is true because the work in this thesis presents a model of the saturated zone in the W2, P1, and corner lot near of the North Unit (Figure 3 and Figure 4). Vadose zone processes are outside of the model domain and cannot be calculated with a saturated zone model. Therefore, all of the processes in the vadose zone that influence groundwater recharge must be estimated without the use of this model, and specified as sources or sinks to the system.

Finally, the data for this study was collected during the drought that began in 2007 and ended in 2009. In the 2007-2008 water year, the field site received approximately 525 mm (25 in) less rainfall than average and the results of this study reflect this.

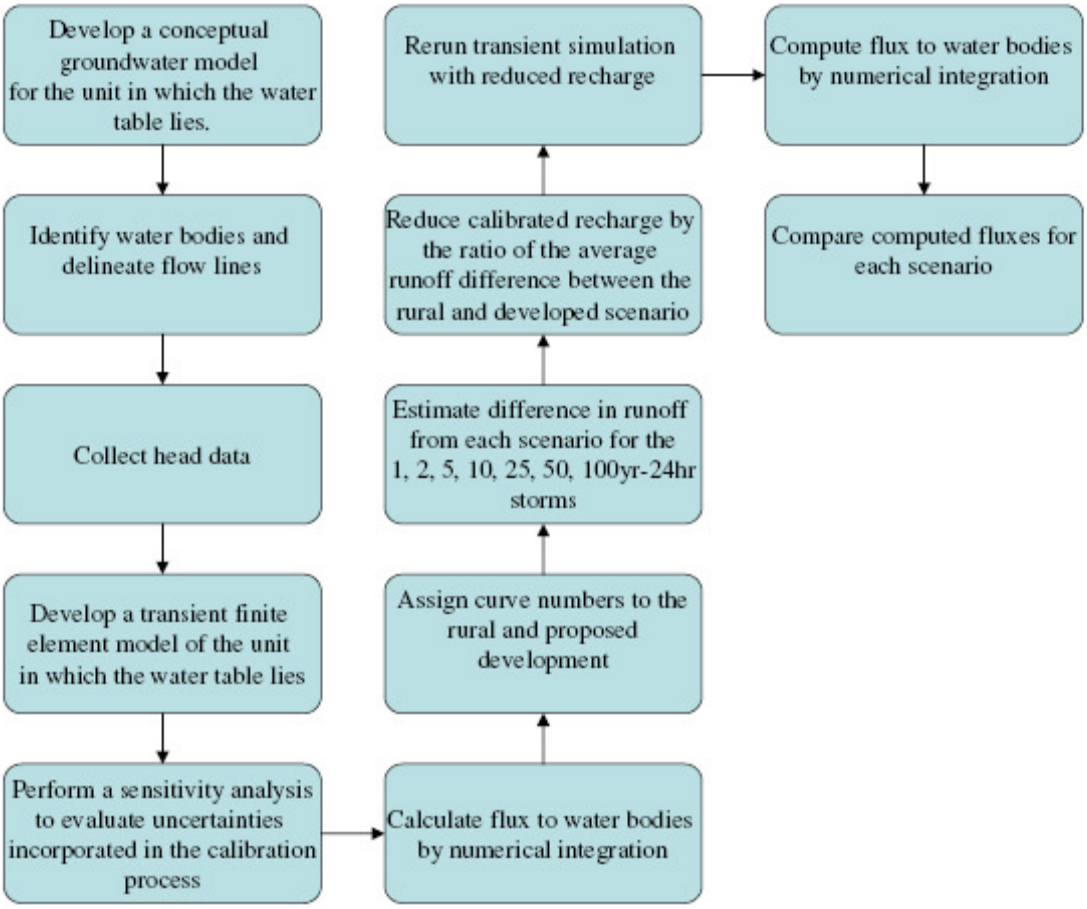

Figure 1: Process flow chart that describes the solution method.

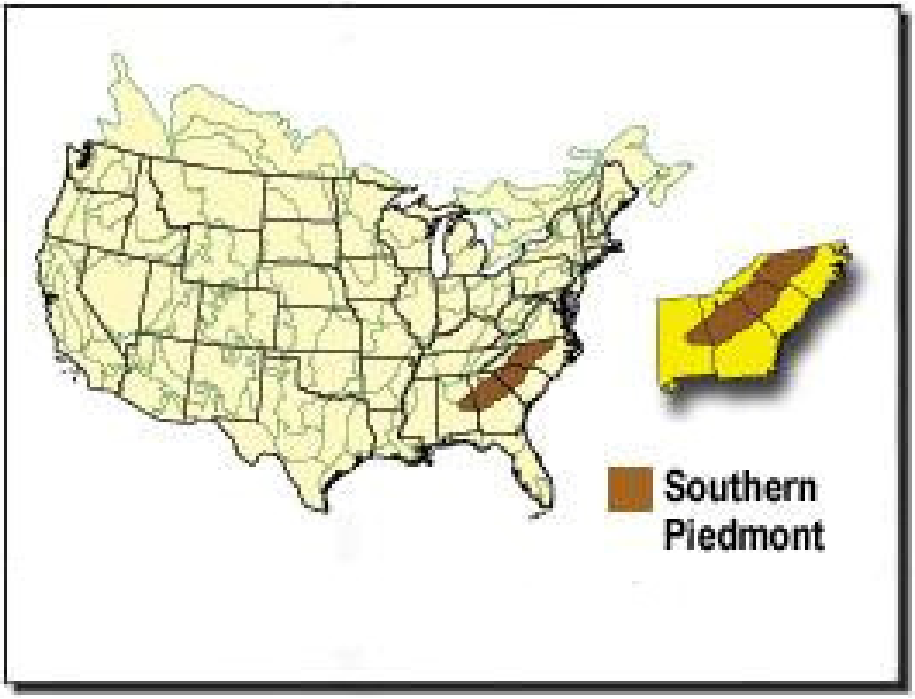

Figure 2: The southern Piedmont Physiographic Region. The southern Piedmont extends through North Carolina, South Carolina, Georgia, and eastern Alabama. (Source: Partners in Flight)

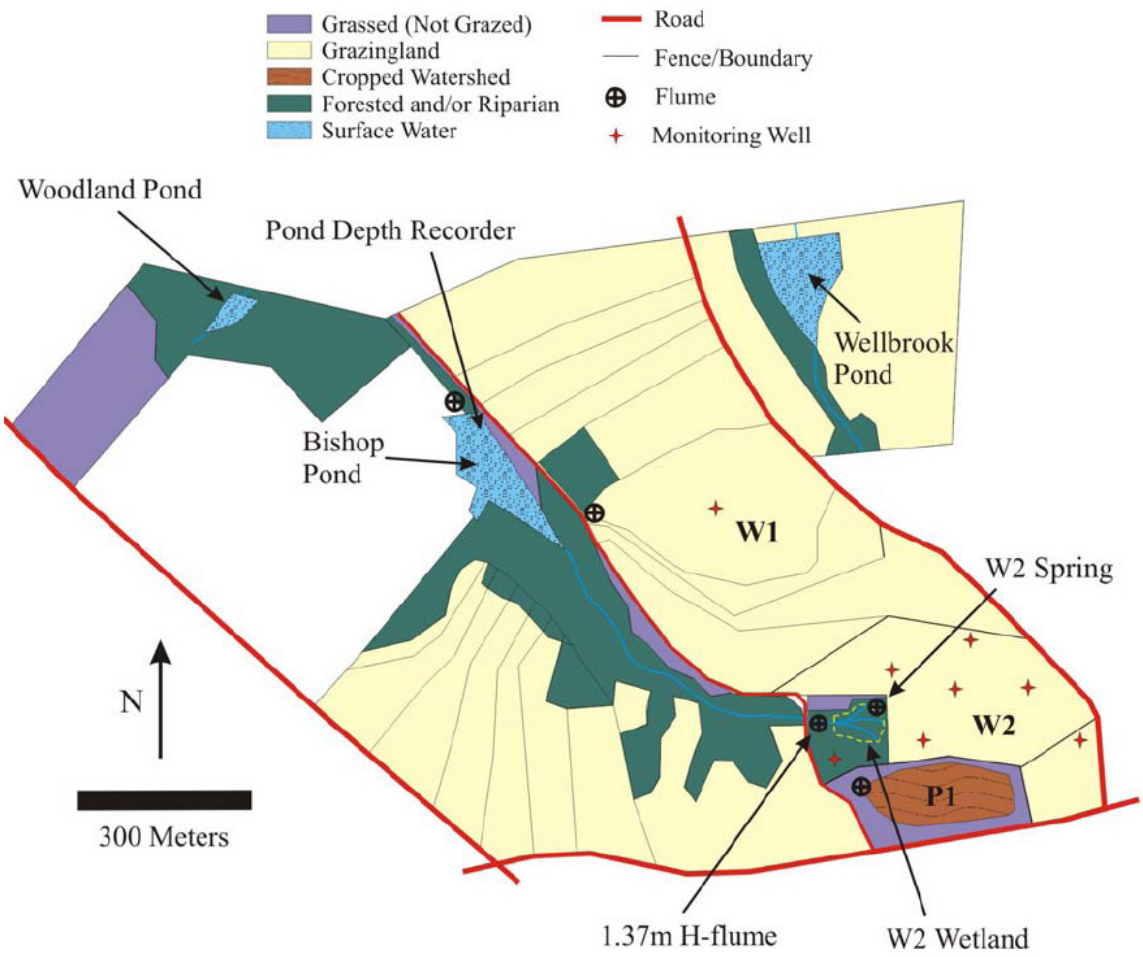

Figure 3: USDA-ARS J. Phil Campbell Natural Resource Conservation Center North Unit. (Source: USDA ARS-JPC)

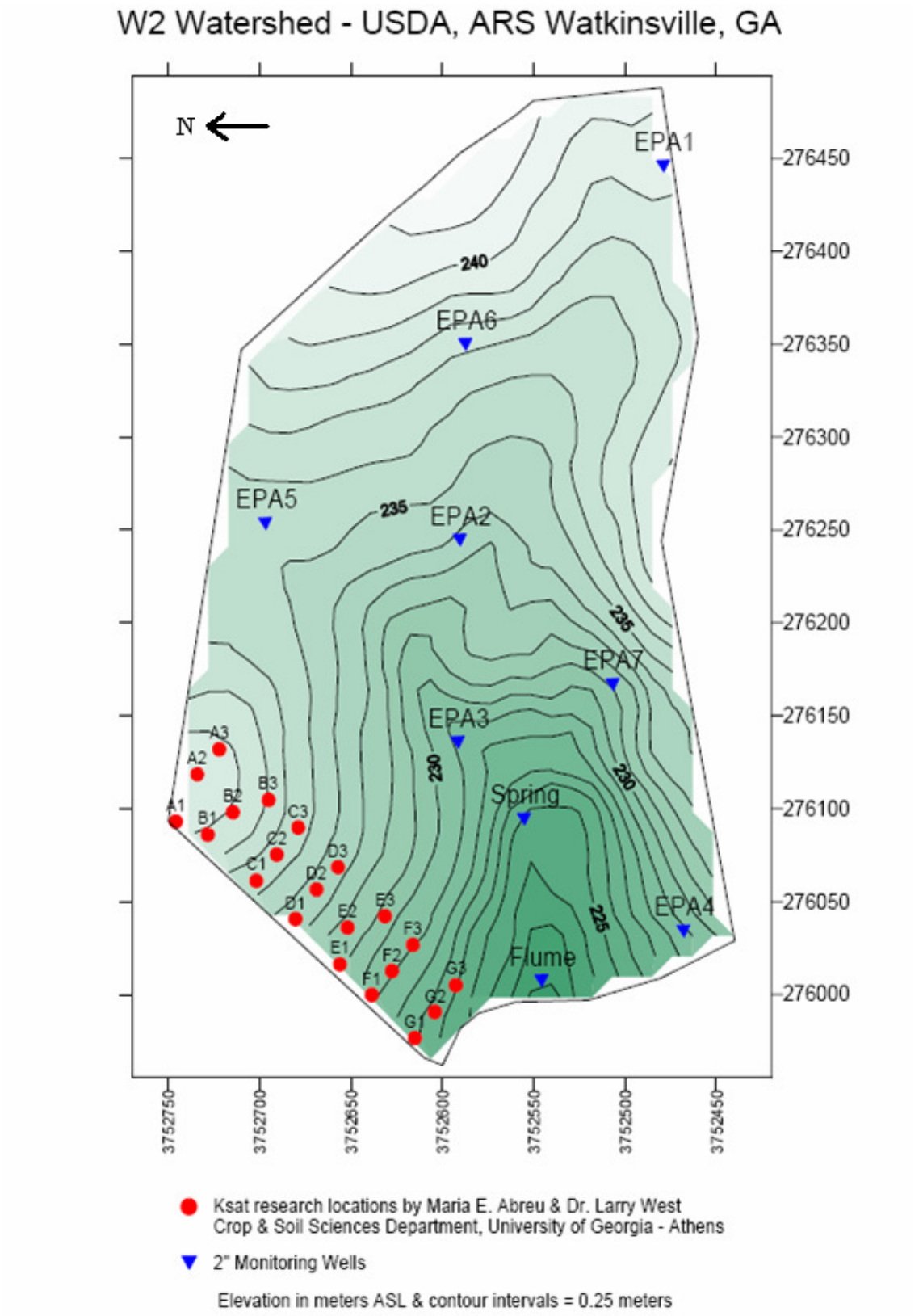

Figure 4: W2 surface contour map with locations of monitoring wells, spring, and 'big flume'. Red dots are Bt, BC horizon Ksat sampling points. (Source: USDA ARS-JPC)

Chapter 2: The Field Site

In the United States, the federal government established a network of geographically distributed experimental watersheds of various sizes throughout the nation in the 1930s. Through adaptation to evolving needs, they have proven to be resources of historic hydrologic data and knowledge. The United States Department of Agriculture, Agricultural Research Service, J. Phil Campbell Sr. Natural Resource Conservation Center (ARS-JPC) is located near Watkinsville, GA (83°24'W, 33°54'N) in the Southern Piedmont (Figure 2). The ARS-JPC property includes land located off of Hwy 129/441 on Hog Mountain Road known as the North Unit. The North Unit encompasses three zero order instrumented watersheds: W1, W2, and P1. The wetland in W2 is the headwater of a small first order stream. The stream flows North West to Bishop Pond and eventually drains to the Oconee River (Amirtharajah *et al.*, 2002). The study took place in an area that encompasses W2 and P1. Figure 3 and Figure 4 provide a visual of the field site.

2.1 Historical Background

When established in 1939, W1 and W2 had residual vegetated bench terraces constructed several decades earlier by farmers that were used for row crop farming. Terraces were removed in 1957 by spreading the spoil over the immediate area and Bermuda grass was established. Winter annuals such as ryegrass (Lolium multiflorum L.) were used to supplement the summer Bermuda grass grazing after 1960. Grazing usually consisted of about 60–100 cows left in W1 to calve and care for their young from late fall to early spring (mid-November to early March). Any over-seeded rye was grazed along with any other vegetation including supplemental hay. Cows and calves were then moved and the watersheds allowed to recover. A smaller number of

cows and bulls were moved in and out of the two watersheds during breeding season beginning early April until the calving season to graze down recovered Bermuda grass (Endale *et al.*, 2006).

Watershed P1 was developed with earthen borders and runoff instrumentation in 1972-1973 and managed in conjunction with other ARS-JPC experimental field plot watersheds P2, P3, and P4 to study pesticide runoff until 1975 (Leonard *et al.*, 1979). P1 was cropped continuously and managed with no till planting of various crops from 1976 to present (Franzluebbers *et al.*, 2007).

2.2 Soils of W2 and P1

The dominant soils types at W2 and P1 are Cecil and Pacolet sandy loam and sandy clay loam (clayey, kaolinitic thermic Typic Kanhapludult (USDA); Chromi-Alumic, Acrisol (FAO, 1998)) derived from the underlying gneiss parent material (Amirtharajah *et al.*, 2002) The Pacolet soils have less thickness (limited A horizon due to extensive erosion) than those of the Cecil series but the properties of the two soils are similar otherwise (Endale *et al.*, 2006). Surface horizons generally are brownish gray sandy loam to red clay loam and overlay red clayey argillic horizons.

West *et al.* (2008) report higher saturated hydraulic conductivity (Ksat) in well developed horizons. On average, Bt1 horizons had well developed structures and a Ksat of 8.2e-4 mm/s compared to poorly developed BC horizons with a Ksat of 1.9e-4 mm/s. Robertson (1968) describes these soils as deeply drained with moderate permeability. Perkins (1987) reports a chemical characterization of the Cecil soil series of Oconee County. The deep well drained moderately permeable soil is generally increasingly acidic with depth. The clay content of this soil peaks in the Bt horizon and reaches a minimum in the C horizon. The cation exchange

capacity of the A, E, Bt1, Bt2, Bt3, and C horizons are 8.9, 6.3, 14.1, 14.2, 11.1, and 9.4 meq/100g, respectively, for a pedon sampled in Oconee County.

2.3 Climate

Long-term mean annual precipitation is 1250 mm (49.21 in) and mean annual temperature is 16.5 °C (61.7 °F) (Hoogenboom, 2009). The area has a temperate climate, long growing seasons, and typically ample rainfall. The Georgia Weather Automated Environmental Monitoring Network webpage (http://www.griffin.uga.edu/aemn/cgi-bin/AEMN.pl?site=GAWH&report=hi) provides details of some pertinent climate data. Average high and low daily temperature in the summers (June through August) of 2007 and 2008 ranged between 31.17 °C (97.10 °F) and 18.31 °C (64.95 °F) in 2007 and 32.94 °C (91.29 °F) and 18.89 °C (66.00 °F) in 2008. Average daily temperatures in the winters (December through February) of 2007 and 2008 ranged between 15.54 °C (59.98 °F) and 0.56 °C (33.01 °F) in 2007 and 15.87 °C (60.56 °F) and -0.5 °C (31.10 °F) in 2008. From 1945 to 2003, average yearly rainfall at Ben Epps Airport in nearby Athens was approximately 1270 mm (50 in) (Anonymous, 2009). However, drought created a rainfall deficit for this study's duration. Total rainfall for 2007 and 2008 was 784.1 mm (30.97 in) and 884.17 mm (34.81 in) respectively. Table 1 provides a summary of climate data.

2.4 Geology and Hydrogeology

LeGrand (2004) characterized the topography of the Piedmont as gently rolling hills with streambed to ridge topographic relief ranging from 22.86 m to 60.96 m (75 ft to 200 ft). The Piedmont slopes to the south and east with a slope of about 4 ‰.

Table 1: Climate Data for the Watkinsville area.

Climate Averages Watkinsville and Surrounding Areas									
	Average High (°C)			Average Low (°C)			Total Precipitation (mm)		
Time Period	1945-2003*	2007**	2008**	1945-2003*	2007**	2008**	1945-2003*	2007**	2008**
Jan	11.39	13.03	11.02	0.72	1.89	-0.50	119.13	88.90	70.61
Feb	13.72	13.59	15.87	1.89	0.56	2.12	112.52	78.23	102.11
Mar	17.78	21.93	19.06	5.39	7.42	4.72	133.60	90.93	81.03
Apr	22.89	22.48	22.25	9.72	7.92	9.02	96.01	39.37	80.26
May	27.00	28.16	26.82	14.39	12.79	13.66	103.89	33.53	65.53
Jun	30.39	32.66	32.94	18.61	18.31	18.89	104.90	37.59	33.78
Jul	31.78	30.91	32.36	20.61	19.58	19.57	124.21	88.14	76.45
Aug	31.22	36.17	31.76	20.11	21.88	19.85	89.66	46.23	97.03
Sep	28.00	30.67	28.10	17.00	17.66	17.06	92.46	24.13	5.59
Oct	23.00	25.39	22.22	10.50	11.98	9.19	78.99	52.07	115.06
Nov	17.50	18.67	16.11	5.28	3.28	2.64	92.71	59.94	70.10
Dec	12.50	15.54	14.29	1.61	3.97	3.48	98.81	147.57	86.61
Year	22.28	24.10	22.73	10.50	10.61	9.98	1246.6	786.64	884.17

*Anonymous (2009)

**Hoogenboom (2009)

Hack (1989) stated that most of the Piedmont is underlain by igneous and metamorphic rock ranging from the Precambrian to late Paleozoic. At the study area, the parent rock is metamorphic gneiss (Railsback *et al.*, 1996). The bedrock is overlain by a regolith of saprolite. A transition zone of course fragments of partially weathered bedrock may appear between the saprolite bedrock interface, which can be a fast path for groundwater and contaminants (Daniel and Dahlen, 2002)

LeGrand (2004) provides a two-part system conceptual model of the hydrogeology for the Piedmont (Figure 5). Most recharge can be attributed to rainfall, which percolates down to the watertable, usually within the saprolite, although it can exist in the bedrock at points where the bedrock is close to the ground surface. In W2 and P1, the uppermost aquifer flow is through the saprolite which ranges from a minimum of eight to a maximum of 21 meters deep (Washington *et al.*, 2006). The saprolite acts as a storage reservoir for fractured bedrock. Some water discharges to surface water bodies and other water is lost to evapotranspiration in lowland areas (LeGrand, 2004).

Washington *et al.* (2004) estimated the hydraulic conductivity of the saprolite within W2 to be 18.6 mm/day to 25.2 mm/day (10^{-5} cm/sec). To do so, they used Jacob straight-line method (Cooper and Jacob, 1946). on data collected from well EPA 3 (Figure 3), which is eleven meters long, fully penetrates the saprolite, and screened from 9 to 11 meters.

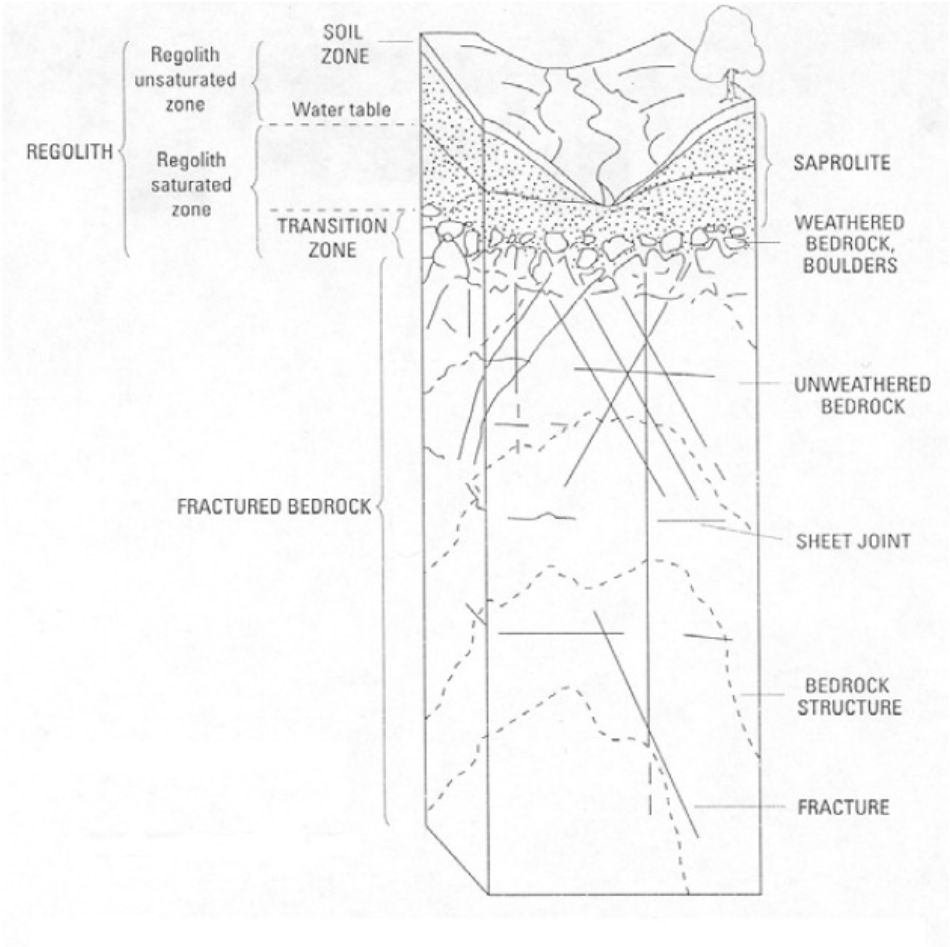

Figure 5: Two-part aquifer system for the Piedmont (Source: LeGrand, 2004)

Chapter 3: Literature Review

Groundwater flow in a particular scenario can be determined by solving a well-posed problem. A problem is considered well posed if it satisfies three requirements: (1) The solution exists, (2) the solution is unique, and (3) the solution depends continuously on the data (Courant and Hilbert, 1989). In groundwater modeling, this consists of a mathematical description of a physical process that includes a governing equation, a domain with boundary conditions, and, for time dependent problems, initial conditions. Discussion of the governing equation and the mathematical statements of boundary conditions applied to this work is reserved for chapter five. The first part of this chapter reviews published findings relating to groundwater flow behavior in saprolite-crystalline bedrock aquifers; the main aquifer system in the Piedmont, Blue Ridge, and Glaciated Northeast physiographic provinces. The first part of the literature review will be used as a guide in choosing proper boundary conditions for the problem. The second part reviews urban recharge studies and published methods for determining groundwater recharge that were applied to this work.

3.1 Conceptual Model

LeGrand (1989) characterizes the Piedmont as a hill and dale topography that the watertable mimics, only with less relief, as shown in Figure 6. Fractured crystalline bedrock is overlain by chemically weathered bedrock, known as saprolite, in which the watertable is usually located. The properties of each part of the system differ though. Saprolite has higher porosity than fractured bedrock but has a smaller affinity for transmitting water than bedrock fractures. Therefore, the saprolite and fractured bedrock aquifer system can be thought of as a reservoir and

pipe system, where saprolite acts as the reservoir and the fractures in the bedrock act as the pipes, although water from saprolite and fractured bedrock are the sources of baseflow water. LeGrand depicts the Piedmont groundwater system as a series of groundwater catchments that discharge in the valley in the form of a perennial stream or a spring that are separated from other groundwater catchments by a groundwater divide at the topographically high ridge. It is worthwhile to note that LeGrand states that his conceptual model is only valid under steady-state non-pumping conditions. Recharge to the groundwater system is in the form of precipitation, which mainly occurs as rainfall.

Schumak (1989) states that there is direct connection between the fractured bedrock and overlying saprolite, and that the two units act as a single aquifer. Schumak investigated the role of fracture orientation on groundwater movement at a site in the North Carolina Piedmont and found that groundwater movement is controlled by the gradient in the direction of large rivers. This indicates that perennial rivers can be continuous groundwater sinks. Champion (1989) presented data that shows the direction of groundwater flow, hence gradient, in fractured bedrock is towards a stream. Champion's data also illustrates that the saprolite and bedrock are in direct connection, and thus, act as one unit.

Nelson (1989) investigated the hydraulic relationship between fractured bedrock aquifers and major streams in Cabarrus County, located in the North Carolina Piedmont. Nelson states "That groundwater flow in the watertable aquifer is along hydraulic gradients that generally conform to topography." This is similar to the way LeGrand (1989) depicts the Piedmont groundwater system. He noted that traditional porous media groundwater models support the concept that surface water bodies act as a discharge boundary for the local and regional ground water system. He also noted that the concept had not been thoroughly tested in a fractured

bedrock hydrogeologic system. A series of multilevel piezometer clusters were installed adjacent to the Rocky River in Cabarrus County North Carolina to measure heads in the saprolite and bedrock. Heads measured in the piezometer clusters were consistently higher than the height of the river indicating that groundwater in the regolith and bedrock adjacent to the river discharged into the Rocky River. His findings support the idea of small individual catchments or local groundwater basins in the Piedmont province.

Groundwater data collected by McFarland (1989) at a site in the Maryland Piedmont indicated that groundwater flow in both saprolite and the schist it overlaid flows from the site to a spring that acts as the discharge point. The direction of flow in the saprolite was primarily horizontal near the watertable although some water leaks down at the base of the saprolite into the underlying schist. At the down gradient portion of the site near the discharge point, water flowed upward from schist into the saprolite.

In the 1960s, Toth worked with sandstones and siltstones in western Canada that formed a near parallel ridge and valley system. He was interested in the role of watertable shape on the groundwater flow patterns within the region. Toth (1962) developed an analytical solution for a two dimensional in profile (x,z) groundwater flow problem. Two simulations were performed with different watertable configurations (A straight line with a gradual slope that mimics topography of the coastal plane, and a sine function that mimics the topography of the Piedmont) on an isotropic and homogenous domain. Toth (1963) stated that the sinusoidal nature of the ridge and valley topography results in three types of flow systems: Local, Intermediate, and Regional. The local system was defined by a recharge area (a topographic high) and a discharge area (topographic low) that were adjacent to one another. Therefore, flow is directly from the recharge area to the discharge area. The intermediate system is a system where one or more

recharge or discharge areas between the topographic high and topographic low are bypassed by some flow paths that flow underneath the local system. Toth (1963) defines the regional system as the flow system that connects the highest and lowest elevations. The highest and lowest elevations are the recharge and discharge areas and flow paths that connect the highest and lowest elevations bypass the intermediate and local systems. Figure 7 illustrates the three flow systems presented by Toth (1963).

Under the flow system conditions, Toth (1962) states that no areal confined systems can exist, and vertical impermeable boundaries or groundwater divides will exist at the highest and lowest topographic elevations, and that these divides will be symmetry boundaries.

The findings of Freeze and Witherspoon (1967) agree with Toth's findings. They present numerous numerical solutions to the three dimensional flow problem under more realistic watertable and permeability configurations. One solution presented by Freeze and Witherspoon (1967), which is in agreement with Toth's solution, is illustrated in Figure 8. Possible flow paths are presented for a hill and valley watertable configuration (similar to the Piedmont's) with layered heterogeneous media.

It is worthwhile to note that Toth's (1963) and Freeze and Witherspoon's (1967) findings (Figure 7 and Figure 8 respectively) support the idea of using a two dimensional planar geometry for modeling groundwater upgradient of the valley in the Piedmont. Downward flow that represents recharge occurs at the topographically high sections of the profile. Flow then diverges into the various groundwater flow systems. The storage capacity of saprolite is much higher than that of the bedrock, and therefore, any water lost to the bedrock is negligible.

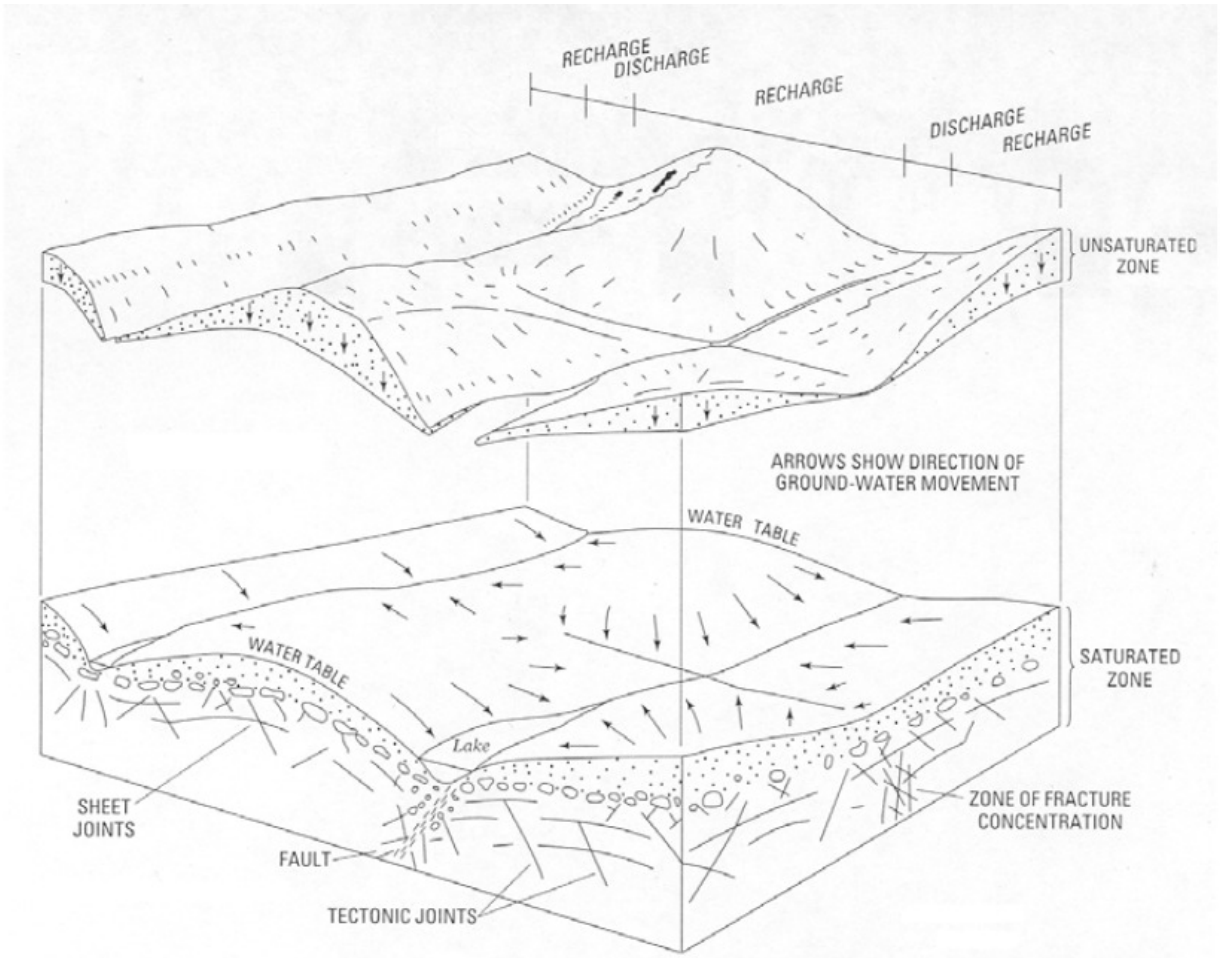

Figure 6: Expanded view of the Piedmont conceptual groundwater flow model illustrating how the watertable mimics the ground surface (from LeGrand, 2004)

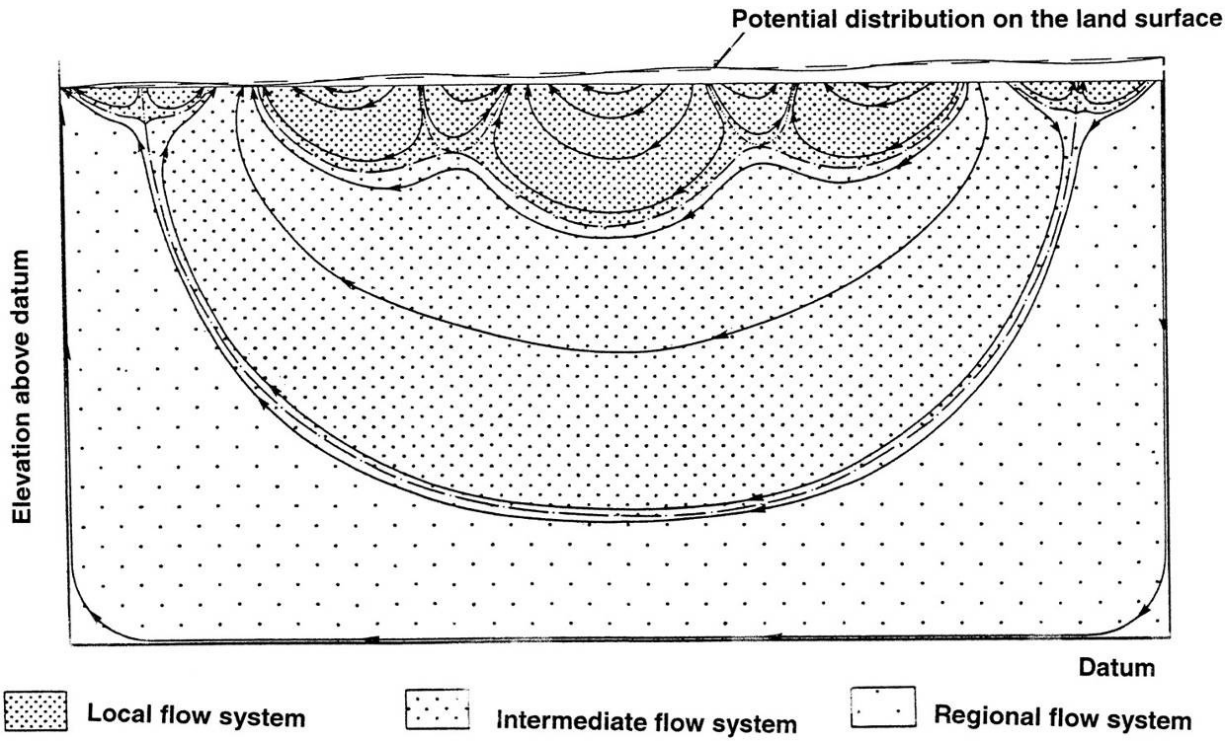

Figure 7: Schematic illustration of local, intermediate, and regional groundwater flow systems. (Toth, 1963)

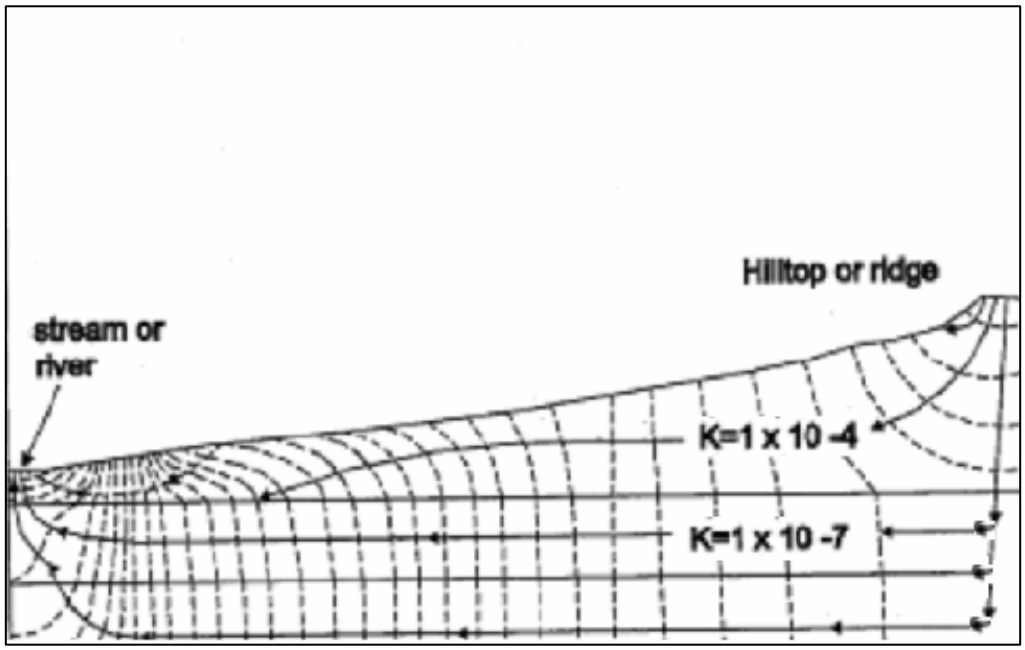

Figure 8: Profile view of groundwater flow in an area where the watertable shape is controlled by land surface expression. Solid lines are flow lines, dashed lines are equipotentials (adapted from Freeze and Witherspoon, 1967).

3.2 Quantification of Groundwater Recharge

In the literature, there are four main methods of estimating groundwater recharge: (1) Tracking changes in soil moisture over time using soil moisture budgets (SMB); (2) adjusting parameter values of groundwater flow models; (3) Multiplying temporal water level fluctuations in wells by the specific yield of the aquifer material and; (4) base-flow analysis of streamflow records. The publications reviewed in this section use some or all of the fore mentioned methods which were adapted to this study.

Erickson and Stefan (2009) developed a soil moisture budget for a 4.6 square kilometer watershed in the Vermillion river watershed in Minnesota to analyze changes in direct recharge in four scenarios of urbanization: Past, present, plus 50 years, and plus 100 years. The moisture budget kept track of water transfer processes and rates in a soil column that extended to the root depth of vegetation. The moisture budget took the form:

$$\Delta S_i = I_i - ET_i - R_i \qquad (3.1)$$

Where:

ΔS_i is the change in storage at time i (mm/day)

I_i is infiltration at time i (mm/day)

ET_i is evapotranspiration at time i (mm/day)

R_i is recharge at time i (mm/day)

In this form, all water entering the soil surface is positive, and water that leaves the system by evapotranspiration or drains past the root zone depth, and becomes recharge in this model, is negative. The ET and I components of equation 3.1 were estimated using three different methods from the literature: (1) FAO-SCS; ET was estimated using FAO-56 (Allen *et al.*, 1998), and I was estimated by subtracting runoff estimated using TP-149 (Kent, 1973) from

precipitation; (2) FAO-GA; ET was estimated again using FAO-56, and I was estimated using the Green-Ampt method (Green and Ampt, 1911); and (3) GA; ET and I were estimated using the Green-Ampt method.

Each parameter in equation 3.1 is dependent on soil moisture. To track the soil moisture, the change in storage in equation 3.1 needed to be related to soil moisture or saturation level. The product of the saturated porosity of the soil and the root zone depth is the depth of water required to completely saturate the root zone. The change in saturation level at each time was estimated by dividing the change in storage by the depth of water required to completely saturate the root zone:

$$\frac{ds}{dt} = \frac{I_i - ET_i - R_i}{\theta_s d_r} \qquad (3.2)$$

Where:

$\frac{ds}{dt}$ is the change in soil saturation (mm/day/mm)

I_i is the infiltration at time i (mm/day)

ET_i is evapotranspiration at time i (mm/day)

R_i is recharge at time i (mm/day)

θ_s is the saturated soil moisture content (mm/mm)

d_r is the root zone depth (mm/day)

Soil water depletion can also be used to represent soil water storage. Soil water depletion is defined as the depth of water required to bring the soil to field capacity, or the water content held in the soil against the force of gravity (Allen *et al.*, 1998). The soil moisture content is related to soil water depletion by:

$$\Theta_i = \Theta_{fc} - \frac{D_{w,i}}{d_r} \qquad (3.3)$$

Where:

Θ_i is the soil moisture content at time *i* (mm/day/mm)

Θ_{fc} is the soil moisture content at field capacity (mm/day/mm)

$D_{w,i}$ is the soil water depletion at time *i* (mm/day)

d_r is the root zone depth (mm)

The soil water depletion was estimated after each time step with:

$$D_{w,i} = D_{w,i-1} - I_i + ET_i + R_i \geq 0 \qquad (3.4)$$

Where:

$D_{w,i}$ is the soil water depletion at time *i* (mm/day)

$D_{w,i-1}$ is the soil water depletion from the previous time step (mm/day)

I_i is the infiltration at time *i* (mm/day)

ET_i is evapotranspiration at time *i* (mm/day)

R_i is recharge at time *i* (mm/day)

All three models used equations 3.2 and 3.4 to estimate soil moisture for parts of the water budget, and each tracked the soil moisture for a full year to determine annual recharge.

Two methods were used to estimate recharge. In the FAO-SCS and FAO-GA models, recharge was calculated by rearranging the water budget equation and using the soil water depletion parameter to in exchange for the change in soil storage:

$$R_i = I_i - ET_i - D_{w,i-1} \geq 0 \qquad (3.5)$$

Recharge was calculated in the GA method by assuming the vertical hydraulic conductivity of the soil was equal to recharge only when the soil moisture was above field capacity. The equation for unsaturated hydraulic conductivity was given by Brooks and Corey (1964):

$$q_p = K(s) = K_s s^{(2+3m)/m} \qquad (3.6)$$

Where:

q_p is the recharge rate (mm/day)

K is the unsaturated hydraulic conductivity (mm/day)

s is the soil saturation (mm/day/mm)

m is the Brooks and Corey pore size distribution (unitless)

The watershed was broken up into soil/land use combinations on a geographical information system. Solutions to equation 3.2 and 3.4 were calculated with a visual basic macro in excel that iterated each of the equation's components with a time step of one day for 365 days.

Each model (FAO-SCS, FAO-GA, and GA) produced similar results. The results showed that natural groundwater recharge decreased from around 20% of the seasonal average rainfall (800 mm) at 4.9% impervious area to around 12% of seasonal average rainfall at 36.4% impervious area (a 30% to 40% reduction in natural recharge). Natural recharge also decreased in suburban settings where native vegetation was replaced with lawns and gardens that increased the ET term. Lerner (2002) points out that the soil moisture budget technique to determine recharge is probably only useful at small scales. Scanlon *et al.* (2002) refers to the SMB method as a residual method. Parameters are measured or estimated and the difference, or residual, of the parameters is the recharge. Therefore, the accuracy the estimated recharge is susceptible to the inaccuracy of parameter estimations.

The second method used in the literature is adjusting parameter values of groundwater models to infer recharge. Yang *et al.* (1999) developed a holistic approach to establishing the spatial and temporal amounts of the three urban recharge sources (precipitation, water mains, and sewers) within the Nottingham (UK) urban aquifer. A calibrated transient groundwater flow model that spanned 1850 to 1995 was supplemented by a solute balance model (advection-dispersion model). Both models' domains were exactly the same.

Their methodology was to calibrate a groundwater flow model of Nottingham by adjusting recharge to match heads. The recharge term used in the model was an "all inclusive" term that took the form:

$$\text{Recharge} = (R_p F_d F_w) + (R_{urf} F_d) \qquad (3.7)$$

Where:

R_p is recharge from precipitation (mm/yr)

F_d is a factor related to superficial cover (unitless)

F_u is a for industrial and urban cover (unitless)

R_{urf} is recharge from urban return flows (sewer mains, water mains, etc…) (mm/yr)

Each component of recharge was assigned a concentration value of the solutes Cl, SO_4, and total N. Each component was adjusted in order to calibrate the solute concentration (advection-dispersion) model of the same domain to match concentrations of each solute measured in the field at particular locations and head at similar locations. They concluded that direct recharge from precipitation had decreased from 179 mm/yr in 1850 to 53 mm/yr in 1995. Leakage from water and sewer mains increased (from 59 mm/yr in 1850 to 158 mm/yr in 1995). However, they also state that the confidence intervals associated with their estimations of sewer and water

main contributions to recharge are $\pm 40\%$ and $\pm 100\%$ respectively, which they attribute to the lack of quality historical data.

Another work that employed a holistic approach was by (Ku *et al.*, 1992). They used a water budget analysis when determining the affects of engineered urban storm-runoff controls on groundwater recharge in Nassau County, Long Island, New York, a primarily residential area (five or ten dwellings per acre) approximately 264 square miles. In the 1940s, recharge basins were engineered in the inland portions of the island as a way to retain the increased runoff caused by urbanization and replenish the surficial aquifer. Runoff near the coast was captured in storm sewers and routed to the ocean. A groundwater model was developed to evaluate the effect of the recharge basins and discharge to streams in terms of the seasonal and spatial distribution of recharge, among other things. Recharge values for pre-development conditions were calculated using a water budget of the form:

$$RE = P - OR - ET \qquad (3.8)$$

Where:

RE is groundwater recharge (mm/day)

P is precipitation (mm/day)

OR is overland runoff (mm/day)

ET is evapotranspiration (mm/day)

The form of the water budget was modified to include seasonal parameter variation:

$$RE_g = P_g - OR_g - ET \qquad (3.9)$$

$$RE_d = P_d - OR_d \qquad (3.10)$$

Where:

RE_g is recharge during the growing season (mm/day)

P_g is precipitation during the growing season (mm/day)

OR_g is overland runoff during the growing season (mm/day)

ET is evapotranspiration (mm/day)

RE_d is recharge during the dormant season (mm/day)

P_d is precipitation during the dormant season (mm/day)

OR_d is overland runoff during the dormant season (mm/day)

Using equation 3.9, recharge in the recharge areas (central Long Island) in post development times were estimated assuming that runoff during the growing season is equal to the increased urban runoff and can be expressed as:

$$RE_g = UR \qquad (3.11)$$

Where:

UR is increased runoff due to urbanization (mm/day)

In the discharge areas near the coast, recharge during the dormant seasons was calculated using equation 3.10. Runoff coefficients that represented the amount of storm runoff in the runoff area and recharge area were calculated by dividing the surface runoff, in inches by the corresponding rainfall, in inches. Runoff in the discharge area was calculated using the hydrograph separation method of Reynolds (1982). Runoff in the recharge area was calculated using values of percentage impervious cover from the literature. These rates were then multiplied by the average precipitation rates of a season to determine average seasonal runoff. Seasonal runoff was then used in equations 3.9, 3.10, and 3.11 to estimate the change in recharge rates for the discharge and recharge areas since pre-development conditions. The findings of this study indicated that no net change in recharge had occurred since the 1940s when recharge basins were constructed, although the spatial distribution of recharge had changed and therefore affected the geometry of

the watertable. Lerner (2002) recommends holistic methods, such as the fore mentioned, for estimating groundwater recharge, although the estimations of each component of urban recharge can suffer from the lack of quality, historical data.

The third method for estimating groundwater recharge found in the literature is to multiply the difference between temporal fluctuations in groundwater by the specific yield of the aquifer. Healy and Cook (2002) term this method the water-table fluctuation (WTF) method. The WTF method is based on the premise that rises in groundwater levels in unconfined aquifers are due to recharge water arriving at the watertable. Recharge can be calculated by:

$$R = \frac{S_y \Delta h}{\Delta t} \qquad (3.12)$$

Where:

S_y is the specific yield ($L^3/L^2/L$)

h is head (L)

t is time (t)

According to Healy and Cook (2002), this method can be used to produce long term seasonal or yearly recharge totals by taking the difference of the yearly high and the yearly low of a well hydrograph.

Healy and Cook (2002) also states that the WTF method does not make assumptions about the pathways by which water travels through the vadose zone, and that the observation well at which measurements are taken are representative of at least several square meters of the study area. In his view, this makes the WTF method a very attractive and simple method to determine groundwater recharge. However, they point out the limitations of the method: (1) the method is best applied to shallow watertables that display sharp water-level rises and declines. (2) The authors state that recharge rates vary substantially based on geology, location, elevation,

surface slope, vegetation, and other factors. The observation well that provides the data which this method is applied to must be representative of the entire watershed. (3) The rate of recharge must be much slower than the rate of water flowing away from the watertable. Otherwise, there would be no change in head. In other words, the drainage away from the watertable must be much slower than the rate of water made available at the watertable, if not, the WTF method will severely under predict recharge. (4) Water levels fluctuate for several reasons. Diurnal fluctuations are often observed where the watertable is close to the soil surface caused by the water needs of vegetation. Changes in atmospheric pressure can cause fluctuations of several centimeters in head, although the combination of long term monitoring data and vented pressure transducer can mitigate error associated with atmospheric pressure fluctuations. Air can become entrapped between the actual watertable and a perched watertable, which would cause a rapid increase in water levels. (5) A wide range of S_y values exists due in part to the heterogeneity of geologic materials and techniques used to measure S_y. Despite the WTF method's shortcomings, Healy suggests that, taken the simplicity of the method and the need to apply multiple estimation methods to recharge, the WTF method should be used whenever possible.

The fourth method for estimating recharge is base flow analysis of streamflow records. Baseflow is defined as "…water that enters a stream from persistent slowly varying sources and maintains streamflow between inputs of direct flow" (Sophocleus, 2002). By and large hydrologists believe that baseflow is mainly supplied by water derived from the aquifer, although many processes (such as contributions from lakes and wetlands that provide water to streams in between periods of rainfall) can contribute water to baseflow under the definition provided by Sophocleus (2002). Baseflow analysis, from a water budget point of view, assumes that all water entering an aquifer is equal to baseflow discharge, which is true under non-pumping conditions.

From this point of view, recharge estimations made from baseflow analysis are necessarily underestimates of recharge because water can be lost through evapotranspiration in riparian zones (Scanlon *et al.*, 2002).

Landers and Ankcorn (2008) evaluated the influence of septic systems on baseflow in Gwinnett County, Georgia, in 24 watersheds of similar size and average slope. Baseflow measurements from 12 watersheds that had high densities of onsite wastewater disposal systems (OWWDS) were compared to baseflow measurements in 12 watersheds that had low densities of OWWDS. Baseflow measurements and other water quality parameters were collected over two days in mid October 2007, during a drought when baseflow constitutes the majority of flow in streams and in a month where evapotranspiration is negligible. After normalizing the data to remove the effect of contributions from estimated water main leakage on baseflow, mean baseflow discharge was found to be 90% higher in areas with a high density of OWWDS than in low density areas because of OWWDS.

Chapter 4: Materials and Methods

This chapter describes the field equipment setup as well as the estimation of potential evapotranspiration, natural groundwater recharge, transmissivity. Model development and calibration, and land use scenarios that were modeled are also described. Chapter five provides the mathematical basis of the groundwater model, along with a description of the computer model Comsol.

4.1 Hydrologic Equipment

The first phase of this project was to gather hydrologic and aquifer hydraulic data at W2. The Environmental Protection Agency (EPA) Environmental Research Division (ERD) works in conjunction with the ARS near Watkinsville, Georgia. Through this partnership, monitoring wells have been installed throughout the ARS property. Many of these wells are located within W2 and were used to collect data relevant to this study (Figure 4). Well specific information can be found in Table 2.

Wells EPA 2, EPA 3, EPA 5, and EPA 7 were outfitted with data logged pressure transducers that measured head continuously for 423 days of the study. EPA 3 was outfitted with a Druck pressure transducer and a Campbell Scientific model CR10 data logger programmed to measure and record feet of head every 15 minutes starting on April 24, 2007. Wells EPA 2, EPA 5, and EPA 7 were outfitted with Odyssey© pressure and temperature data recorders (Model # ODYPS10) that were programmed to measure and record mm of head every 10 minutes starting on September 5, 2007.

Monitoring equipment left over from a previous study by Amirtharajah *et al.* (2002) was utilized to quantify flux out of the wetland. A 0.33 m H-flume was installed to monitor spring flow. A pressure transducer (Model PDCR-1830-8388, Druck Inc. New Fairfield, CT) was inserted into the stilling well and wired to a data logger (Model CR10X, Campbell Scientific) to measure spring flow depth over the flume base.

A large 1.37 m H-flume was past the point of convergence for two streams that flow east to west, one emanating from the main wetland spring and the second from another rather diffused spring 20 m or so south of the main spring. The "big" flume had been outfitted with a pressure transducer (Model PDCR-1830-8388, Druck Inc. New Fairfield, CT) which was wired to a data logger (Model CR10X, Campbell Scientific) to measure depth of flow over the flume base.

A rain gauge (Model TR525M, Texas Electronics, Inc.) had been installed at a nearby location 180 meters SW of the spring near the big flume. The data logger was programmed to take precipitation measurements every ten minutes and calculate cumulative precipitation.

4.2 Estimation of Evapotranspiration, Recharge, and Transmissivity

Potential evapotranspiration (PET) from the wetland was estimated using the Thornthwaite method (Thornthwaite, 1948). Thronthwaite's method is an empirical relationship between monthly mean air temperature and monthly ET that can produce reliable results for areas that are "well wetted". Since the wetland area is well wetted, PET was used rather than actual evapotranspiration (AET) because: (1) Average monthly temperature data was available from a nearby (less than 100 meters away) weather station; and (2) PET and AET are very similar in areas where there is an abundant water supply for vegetation. PET was applied on the torus subdomain (see Figure 10) to represent a direct sink on watertable because the vegetation

root zone is a direct sink to the watertable in that area. PET was not incorporated as a sink at higher elevations in the watershed because the vegetation does not represent a sink to the watertable at higher elevations outside of the wetland. Evapotranspiration is already included in recharge at higher elevations outside of the wetland.

Recharge was estimated by baseflow analysis of the Middle Oconee River near Athens (USGS gauging station 2217475), Middle Oconee River near Arcade (USGS gauging station 2217500), and Murder Creek above Eatonton (USGS gauging station 2221525), using a local minimum method similar to the one utilized by the HYSEP program developed by the United States Geological Survey (Sloto and Crouse, 1996). On average, baseflow analysis of these watersheds indicated that yearly groundwater recharge was about 11.6 mm/water year (0.4 in/water year). The hydrographs reflect the drought that persisted throughout this study, and therefore, recharge is biased towards the lower extreme.

In addition to baseflow analysis, the WTF (see section 3.2) method was applied to data from well EPA 2. EPA 2 was chosen because of its position within the watershed and because the data, when plotted, was much smoother the data collected from any other wells that were outfitted with pressure transducers. Using a value of 0.05 for specific yield (the model calibrated specific yield) WTF analysis of the well hydrograph at EPA 2 indicated that recharge was about 32.76 mm/water year (1.29 inches/water year). The recharge estimations obtained from baseflow analysis and WTF analysis were used as the lower and upper bounds on the recharge input for the model.

Both recharge methods produced recharge values that were much lower than what would be expected. Underestimation of baseflow is inherent in the local minimum method procedure. The WTF procedure is highly sensitive to the value of specific yield. Measurements of specific

yield were not available at the site, so the model calibrated value of specific yield was used in the WTF analysis.

The groundwater flow equation for a two dimensional representation of an unconfined aquifer is non-linear, which makes solving the equation very difficult. A simple way of linearizing the equation for groundwater flow in an unconfined aquifer is to multiply hydraulic conductivity by the saturated thickness of the aquifer. The product, called the transmissivity, replaces the Kh term inside second differential (see chapter 5 for a discussion of the linearization techniques for unconfined groundwater flow problems) and linearizes the problem. A range of values for saprolite hydraulic conductivity was taken from works that measured hydraulic conductivity of saprolite within W2 or at the ARS (Overbaugh 1996; Washington *et al.* 2006). The saturated thickness of the saprolite was estimated by using the observed head in the wells EPA 2, EPA 3, and EPA 7 (each of which were augered to refusal and the refusal depth was assumed to be the depth to bedrock) on September 10, 2007 (the first day of the simulation) by the following procedure:

$$W_D - (GSE - h) = b \qquad (4.1)$$

Where:

W_D is the well depth (m)

GSE is the ground surface elevation (m asl)

h is head (m asl)

b is the saturated thickness of the aquifer (m)

Saturated thickness at the three locations were averaged and applied over the entire domain and held constant over time. The resultant average saturated thickness was 7.76 m. See

Table 2 for details specific to each well. Figure 9 displays the profile view of the domain with the saturated thickness.

4.3 Development and Discretization of the Model Domain

The domain was chosen in accordance with the conceptual model of groundwater flow in the Piedmont as described in chapter 3. A topographic map was used to identify ridges and flow lines that were assigned no flow boundaries. The wetland and stream area were identified and locations of the thalweg of the wetland and stream. Those locations were imported into Comsol's CAD utility as a solid object. The ridges and flow line locations were then loaded into the CAD utility which produced a solid object that included the full domain, including the wetland and stream. The wetland and stream object was subtracted from the full domain object. This produced several line segments that took the shape of the wetland. Ground surface elevation was known at the endpoints of the line segments. It was assumed that the watertable was, on average, 609.6 mm (two ft) below the land surface in the wetland area. Therefore, 609.6 mm was subtracted from the surface elevations at the endpoint to estimate the average elevation of the watertable at those points. The line segments around the outline of the wetland and stream were assigned constant head boundaries with a linear interpolation function that interpolated between the end points of the line segments. A torus-like subdomain was drawn around the thalweg wetland and stream to the extent of the wetland, and these line segments were assigned internal continuity boundaries. Figure 11 below displays visual for boundary assignments around the domain. A finite element mesh was constructed across the domain that consisted of 22,417 triangular elements. The mesh graded from small elements near boundaries to larger elements near the center of the domain. The Comsol user's manual defines element quality as the aspect ratio and computes the quality of a two dimensional mesh of triangular elements as:

$$q = \frac{4\sqrt{3}}{h_1^2 + h_2^2 + h_3^2} \qquad (4.2)$$

Where:

q is the mesh quality ($1/L^2$)

h_i^2 is the length of side i of an element (L^2)

The mesh quality, q, is a number between one and zero. The Comsol user's manual states that a mesh with a q larger than 0.3 will not affect the quality of the solution. The quality of the mesh used in this work is 0.4971. Figure 12 displays the finite element mesh.

Table 2: Well name, surface elevation, depth, screen interval, and screen material. Each well listed is within W2.

Well Identification	Surface Elevation (m asl)	Well Depth (m)	Screened Interval (M below land surface)	Screen Material
EPA 2	234.437	13.77	8.54 – 11.59	PVC slotted screen
EPA 3	229.131	10.90	7.62 – 10.67	PVC slotted screen
EPA 5	236.395	20.82	18.29 – 21.34	PVC slotted screen
EPA 7	231.426	11.9	5.79 – 11.89	PVC slotted screen

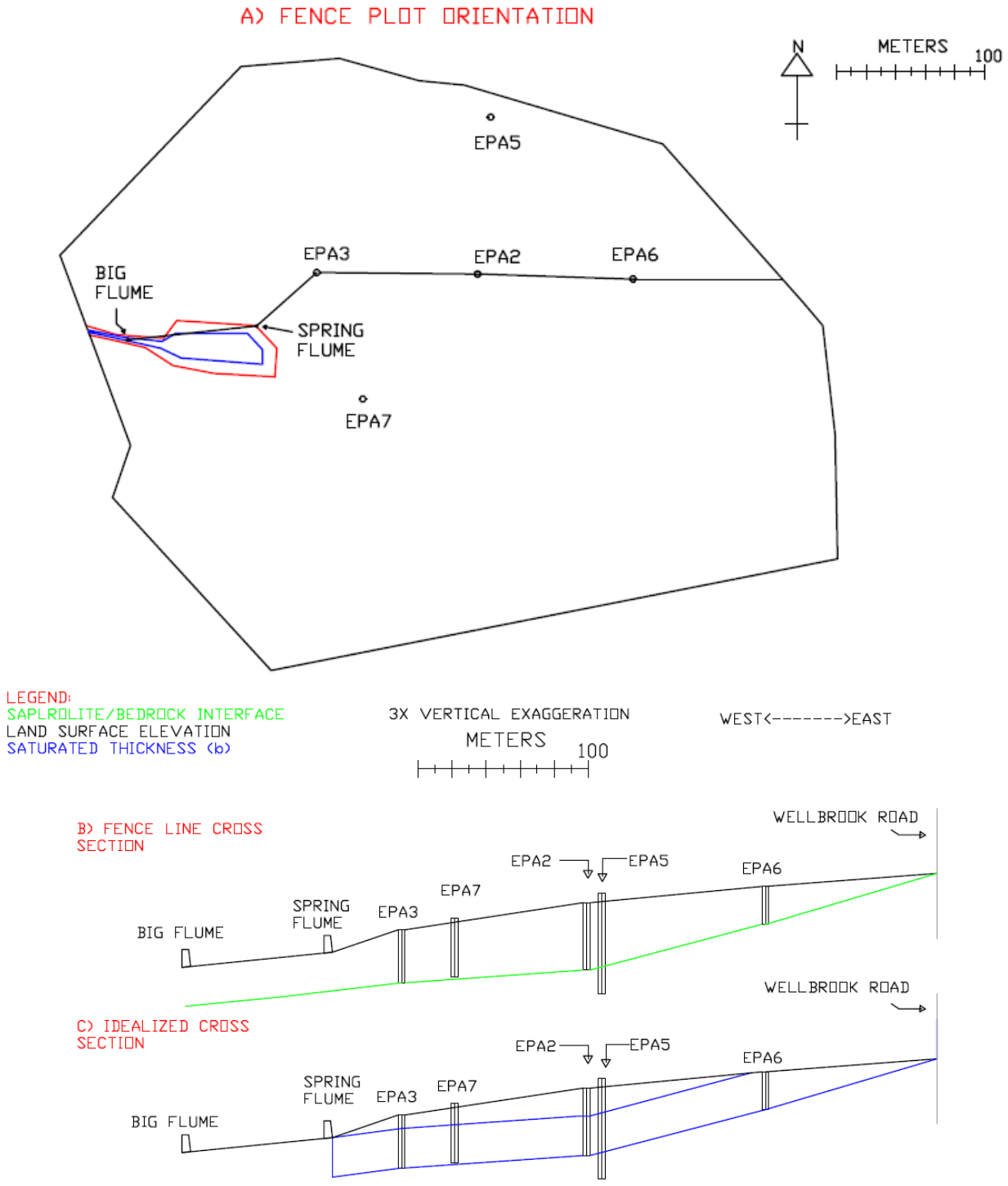

Figure 9: Fence plot of the watershed. Figure 9A displays the fence plot orientation; Figure 9B shows the profile of the fence plot line with depth to bedrock (green line depicts bedrock elevation along transect); Figure 9C shows the profile of the fence plot line with the average saturated thickness (depicted by the blue lines) of the saprolite.

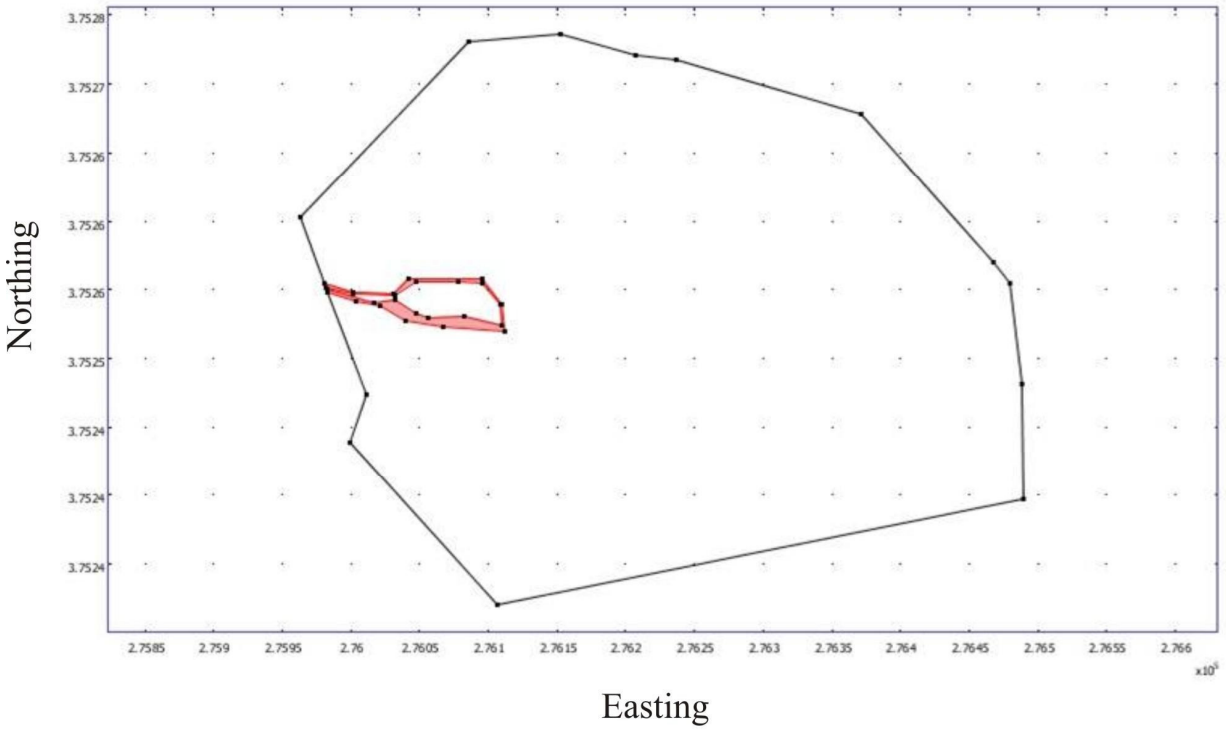

Figure 10: Torus of potential evapotranspiration around wetland

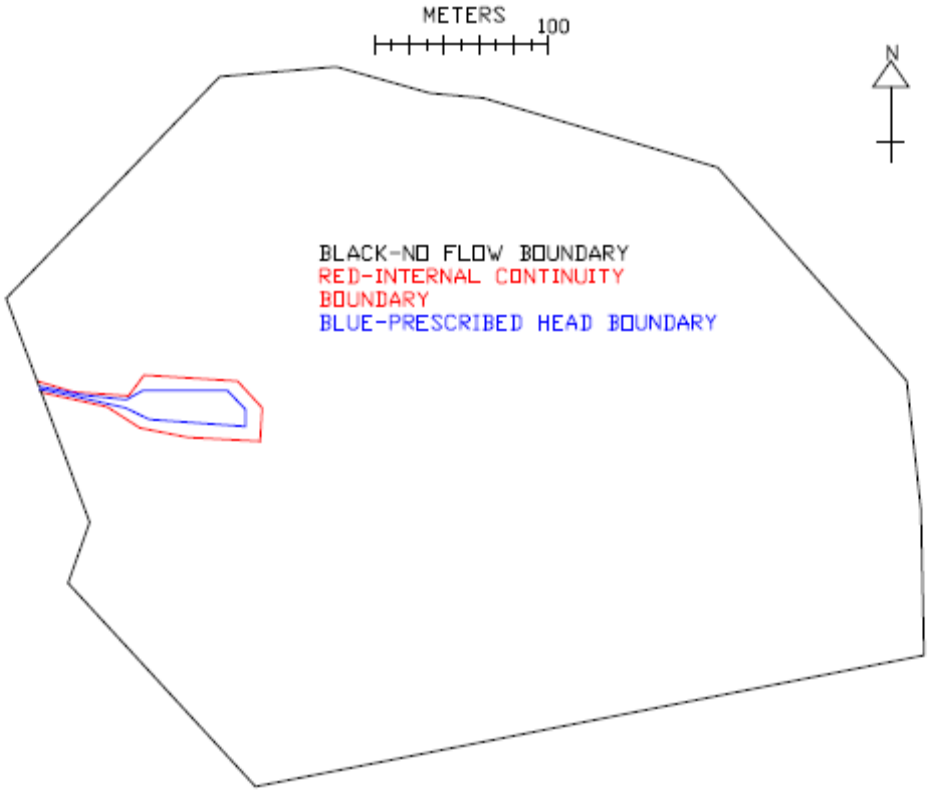

Figure 11: Plan view of the domain with boundary conditions.

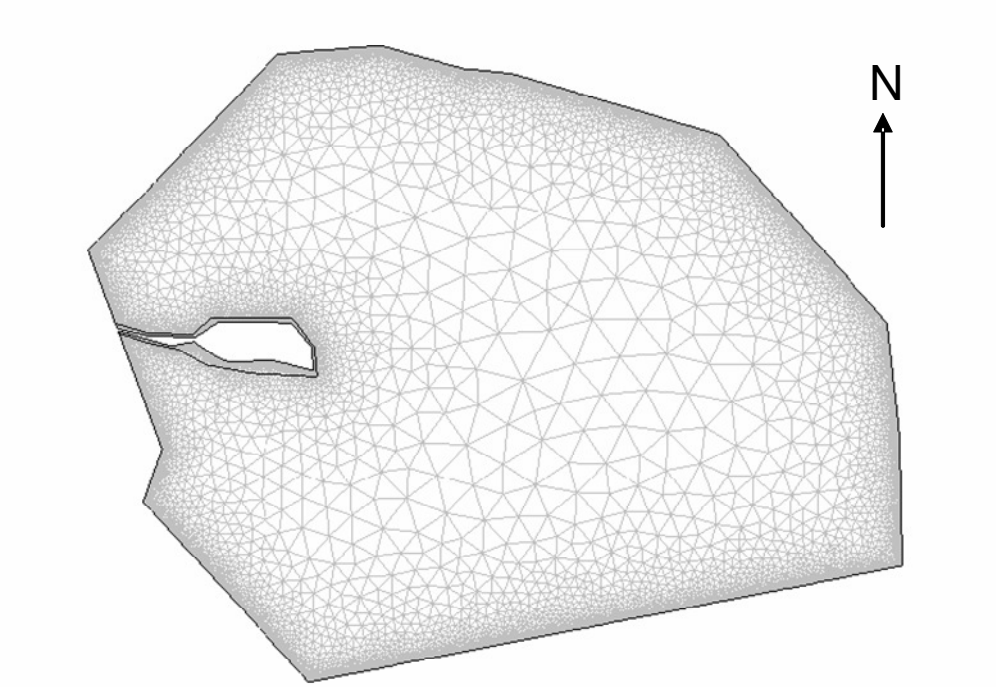

Figure 12: Finite element discretization of the domain

4.4 Steady-state Parameterization and Calibration

In the field of differential equations, an initial value problem is a differential equation together with specified value, called the initial condition, of the unknown function of head at a given point in the domain of the solution. In this research, the calibrated steady-state solution provided the initial conditions (the head distribution everywhere) for the transient simulation

It was assumed that the bedrock surface had the same general slope as the land surface so bedrock slope values were obtained by ground surface elevation measurements of wells within W2. The bedrock slope in radians in the x direction was found by taking the inverse tangent of the elevation and easting differences between EPA 1, the well furthest east in W2, and EPA 3. The bedrock slope in radians in the y direction was found by taking the inverse tangent of the elevation and northing differences between EPA 5, the well furthest north in W2, and EPA 7.

Two parameters were adjusted during the steady-state portion of model calibration: (1) Recharge (mm/day) and (2) hydraulic conductivity (mm/day). Recharge was varied within the range of values determined from baseflow separation analysis and WTF analysis. In order to make heads match within the specified tolerance, the saprolite had to be considered heterogeneous. An interpolation file was created that detailed hydraulic conductivity at the coordinates of four corners of a rectangle that lay over the domain. The hydraulic conductivity values specified at the four corners of the rectangle were obtained from steady-state model calibration and were within the order of magnitude range of measured saprolite Ksat in Washington *et al.* (2004) and Overbaugh (1996) (100 mm/day to 10 mm/day) . Both parameters were varied until model predicted heads were less than 0.1 meters different from observed heads at wells EPA 2, EPA 3, and EPA 7, which was the specified tolerance.

During calibration, model predicted heads could never match head observed at wells EPA 2, EPA 3, EPA 5, and EPA 7 simultaneously. The model could be calibrated to match head at wells EPA 2, EPA 3, and EPA 7, or, model could be calibrated to match head at EPA 5 but not the three other wells. There was also concern that EPA 5 may have been augered through the saprolite somewhere in the bedrock. The EPA 5 installation notes indicated that the well had been augured to refusal then augured another 7.62 m (25 ft) with additional augers. Therefore, observed head at EPA 5 was not incorporated into the calibration. A summary of parameter values for the calibrated run can be found in Table 3 and Table 4.

4.5 Transient Calibration

The calibrated steady-state solution was used as the initial condition to the transient solutions. The transient simulation represented the dynamics of the watertable and groundwater discharge to the wetland over a 423 day period from September 10, 2007, to November 3, 2008. Comsol offers three different procedures for time stepping: (1) Free time stepping, where, if the solution does not change rapidly during the first few time steps, solutions are computed most infrequently and more frequently interpolated between time steps; (2) Intermediate time stepping, where, Comsol recognizes that the solution has changed rapidly over a few time steps and interpolates solutions between time steps less frequently than the free time stepping procedure; and (3) Strict time stepping which ensures that the solution is computed at least one time per user specified time step (one day), and interpolates solutions between time steps the least frequently. The strict time stepping procedure was used in this work to (1) ensure that rapid changes in the solution were not missed because Comsol interpolated the solution between two distant time steps, rather than calculated the solution, and (2) because the strict time stepping produced the smoothest computed well hydrographs.

A piecewise cubic interpolation function was created to vary recharge with time so that the shape of the calculated heads matched the shape of the observations at wells EPA 2 and EPA 7. The computed well hydrographs matched the observed well hydrographs best using a value of 0.05 for specific yield. Data from well EPA 3 was not included in the transient calibration because of issues with the monitoring equipment.

4.6 Land Use Scenarios

Groundwater flux occurs across prescribed head boundaries. An expression for outward normal (into the wetland) flux was integrated across the prescribed head boundary of the wetland thalweg up to the position of the "big flume" after each specified output time (each day) for the 423 day simulation (see Figure 13).

The wetland response was evaluated under five different scenarios: The current land use (here on referred to as the rural scenario); a housing development with leak free water and sewer mains (here on referred to as the urban scenario); a housing development with leaky water and sewer lines (here on referred to as the leaky urban scenario); a housing development in which each house has an onsite a septic tank that provides constant recharge to the aquifer (here on referred to as the septic scenario); and a housing development in which each house has a septic tank that provides constant recharge to the aquifer and a well that supplies water for each household (here on referred to as the septic well scenario).

Table 3: Recharge, PET, saturated thickness, bedrock slope east to west, and bedrock slope north to south used in the steady-state calibrated model.

Parameter	Value
Recharge (mm/day)	2.24E-01
PET (mm/day)	4.215
Saturated thickness (mm)	7760.0
Bedrock Slope East to West (radians)	0.0506
Bedrock Slope North to South (radians)	0.0085

Table 4: Hydraulic conductivity (K) values used in calibrated model at four corners of interpolation grid.

Point	Easting	Northing	K (mm/d)
1	276150	3752400	300.0
2	276200	3752400	700.0
3	276150	3752500	330.0
4	276200	3752500	700.0

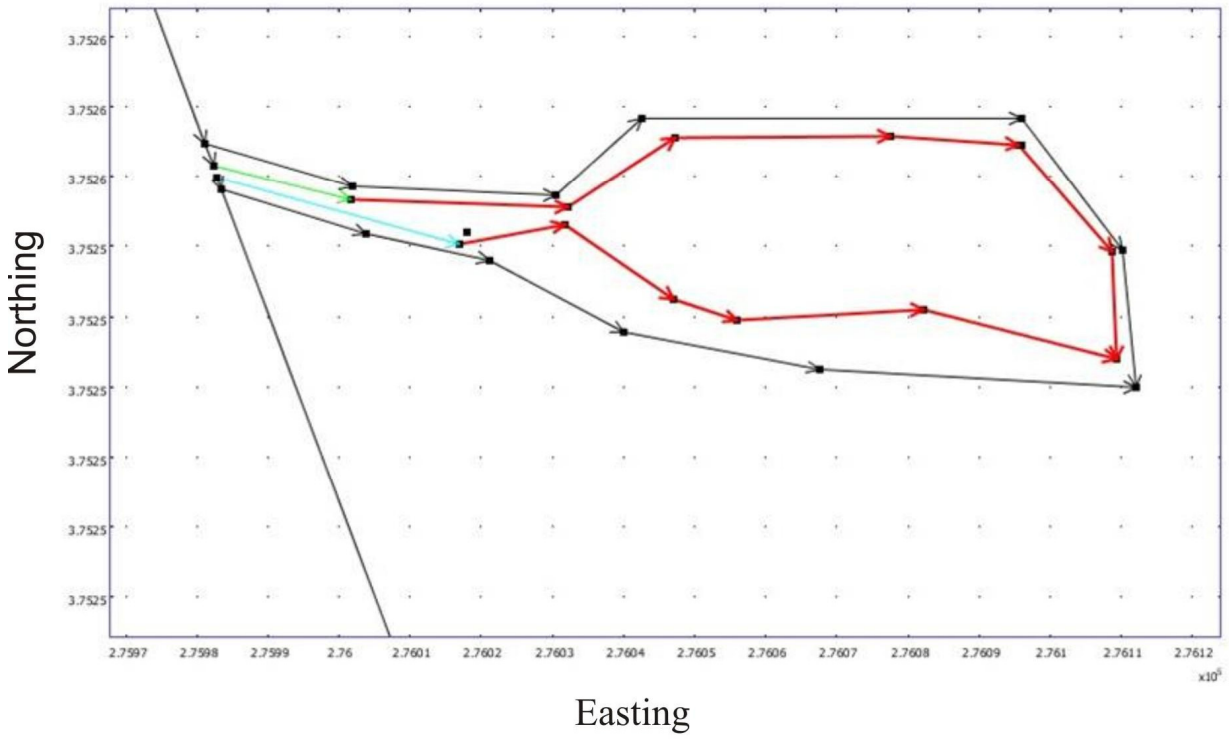

Figure 13: Dirichlet boundaries (in red) that specific discharge was integrated across. The black dot in between the western most red dirichlet boundaries is the location of the "big flume".

4.6.1 Rural and Urban Land Use Scenarios

The rural scenario is the current land use and recharge values for that scenario were obtained from the transient calibration phase. Figure 14 provides a visual of the sites current land use with curve numbers for W2, P1, and the corner field. Table 5 provides a summary of the curve numbers assigned to each area in the rural scenario and the area weighted average curve number assigned to the entire area in the rural scenario.

The urban scenario was a simulation with reduced direct recharge resulting from increased percentage of impervious area associated with a residential housing development. Figure 15 provides a visual of a possible housing development on W2, P1, and the corner field. Table 6 provides a summary of the curve numbers assigned to each area and the area weighted average curve number assigned to the entire area in the urban scenario.

The rural and urbanized land use scenarios were assigned a curve number from the Soil Conservation Services (SCS) Technical Report 55. The Curve Number (CN) method allows direct estimation of total runoff volume, Q, as a depth over the watershed area. A CN represents an area's maximum potential for producing runoff from a given 24-hour total rain event, as determined by regression analysis from extensive runoff studies for various soil and vegetative cover groups. TR-55 has several curves tabulated that are used to estimate runoff from a given area watershed, soil and vegetative cover, and 24-hour precipitation event. Several curve numbers are also tabulated for proposed urbanization of watersheds, which is one of the reasons for using TR-55 to obtain curve numbers in this work. The curve numbers obtained from TR-55 for the two land use conditions were used in the SCS's winTR-20 program to calculate runoff for various storms.

TR-55 was published as a shortcut to the extensive calculations in the SCS's TR-20 program, which computes a storm hydrograph for a given storm. Typically, TR-20 computes runoff more accurately for a given storm, wetland area, and CN than TR-55. The curve number method has been used extensively by planners when designing storm water routing systems for proposed developments. Limitations to the curve number method are: (1) The amount of runoff calculated using TR-20 is very sensitive to the curve number. (2) Limitations to the curve number method is that TR-20 and TR-55 do not predict runoff accurately in forested watersheds that are smaller than 20 acres (Fennessey *et al.*, 2001). (3) Furthermore, TR-20 does not predict runoff well in watersheds with curve numbers that are not within 30 to 100. The first limitation has the most influence on model results out of each of the CN limitations listed (see section 4.7.3 below).

In many engineering designs, watersheds that have several runoff producing soil/land cover types are given an area weighted average curve number. This area weighted average curve number is a composite approach that averages soil/land cover type areas and their curve numbers. An area weighted average curve number was assigned to the rural and the urban land use scenarios.

Storm events are organized by the recurrence interval (in years) for a storm duration (24 hours) in which a depth of rainfall occurs. The precipitation depth for the 1yr-24hr, 2yr-24hr, 5yr-24hr, 10yr-24hr, 25yr-24hr, 50yr-24hr, and 100yr-24hr storm events were taken from the rainfall frequency atlas in TP-40 of the U.S. Weather Bureau (Hershfield, 1961). An additional storm at W2 in March of 2007 was also included. TR-20 was used to calculate the runoff produced by the storm events for the pre-developed and post-developed scenarios. The difference in runoff for each storm was averaged then divided by the number of days over which

recharge was applied in the calibrated transient model (300 days) and calibrated recharge was reduced by 3.331e-2 mm/day on every day that recharge was not zero as a first approximation of natural groundwater recharge in the urbanized scenarios. This was done because: (1) The average difference in runoff exceeds all recharge values specified and zero recharge is not realistic; and (2) a unit increase in runoff does not constitute a unit decrease in recharge, which is best understood with a water budget example. Considering the rural scenario, groundwater recharge can be calculated with a water budget if recharge is assumed to be equal to the difference between infiltration and evapotranspiration:

$$P - (Q_{BF} + Q_{RO}) = R;\ R = I - ET \qquad (4.3)$$

Where:

P is precipitation (L/t)

Q_{BF} is baseflow measured in the big flume (L/t)

Q_{RO} is runoff measured in the big flume (L/t)

R is recharge estimated using the WTF and baseflow separation methods (L/t)

I is infiltration (L/t)

ET is evapotranspiration (L/t)

In the rural scenario, yearly recharge was constrained by baseflow separation and watertable fluctuation method estimates, and does not require estimations of I or ET. However, in the theoretical urbanized scenarios, equation 4.3 is an underdetermined problem, because I and ET are unknowns, both of which must be known to compute recharge in the water budget in equation 4.3. Also, in the urban scenario, it is impossible to constrain a recharge rate because the WTF method requires data from a well on the urbanized site, which does not exist.

Infiltration, evapotranspiration, and soil storage are not part of the groundwater model output. In order to model recharge with those missing components, either a variably saturated groundwater model that calculates recharge as flux across the watertable, or a soil moisture budget model, which calculates recharge residually with estimations of infiltration and evapotranspiration (that are unavailable), must be used. Since the saturated zone model in this work does not calculate recharge; the estimate of natural groundwater recharge in the urbanized scenarios must be considered a first approximation. Runoff differences for each storm for the rural and urban scenario's can be found in Table 7. Figure 16 provides a visual of recharge during the rural and urban scenario.

4.6.2 Leaky Urban, Septic, and Septic Well Scenarios

The leaky urban scenario was a simulation with reduced direct recharge resulting from the increased percentage of impervious surface area associated with a residential housing development with leaky sewer and water lines. In this scenario, 0.90 m^3/day (238.1 gal/day) were pumped to each of the 19 houses. Each household was assumed to use 0.757 m^3/day (200 gal/day). The difference, 0.144 m^3/day (38.1 gal/day), was assumed to be a steady constant source of groundwater recharge. It was assumed that 16% of the 0.757 m^3/day of sewage water produced provided a constant source of groundwater recharge via leaks in the sewer pipes. In total, the leaky water and sewer lines provided a constant steady source of groundwater recharge at a rate of 0.011 m/day over a 25.13 m^2 area within each of the 19 house lots. Figure 17 displays the location of the leaky sewer and water lines.

The septic scenario used the same recharge rate as the urban scenario. Onsite wastewater treatment systems supply constant recharge to the model domain as an area source. Landers (2008) estimated the consumptive use of septic tanks in Gwinnett County, Georgia to be roughly

17% of an assumed 0.757 m^3/day (200 gal/day) use per home. Recharge from the septic tanks was supplied at a constant rate of 0.025 m/day over the area of the septic leach field (25.13 m^2) throughout the 423 day simulation at each of the 18 septic tank locations (see Figure 17 for the placement of the septic tanks in the developed watershed).

The septic well scenario also used the same recharge rate as the urban scenario. In this scenario, septic tanks supply the same constant recharge as the septic scenario. Wells are simulated in the model domain as point sinks that withdraw water from the saprolite at a rate of 0.757 m^3/day (200 gal/day) from the saprolite. Even though all wells that have yields suitable for supplying a single house pump water from bedrock fractures, the water that enters those fractures is stored in the saprolite and the water withdrawn still represents a sink to the saprolite (see section 3.1). Figure 17 shows the locations of wells throughout the developed watershed.

4.7 Sensitivity Analysis

The calibration of this model led to a set of hydrologic parameters that generated a match between observed and computed heads. The objective of a sensitivity analysis is to determine which of theses factors, when changed from the calibrated values, causes the largest change in computed head and computed flux. The allowable range of parameter values for each parameter was limited to the ranges of values from the literature or measured onsite or near the site and summarized in Table 7a. A sensitivity analysis is considered to be an integral part of the modeling procedure (Anderson and Woessner, 1992).

4.7.1 Sensitivity Analysis Methodology for PET, Recharge, and S_y

A first order error analysis was performed. Each parameter was assumed to have a normal statistical distribution. The mean and standard deviation of each parameter distribution were calculated and PET, recharge, and specific yield were varied by ± two standard deviations,

individually, each time the model was executed during the sensitivity tests. The sensitivity analysis was performed at steady-state for potential evapotranspiration and recharge, and at unsteady-state for specific yield.

4.7.2 Sensitivity Analysis Methodology for Transmissivity

A first order error analysis was also performed with transmissivity at steady-state in the same manner as with potential evapotranspiration, recharge, and specific yield. The orientation of the transmissivity field at the field site was also unknown. Therefore, in addition to the incremental changes described above, the transmissivity field (via the calibrated hydraulic conductivity interpolation function) was also rotated clockwise 90° from due west three times. Head and groundwater flux were calculated during each individual run.

4.7.3 Sensitivity Analysis Methodology for Curve Number

A sensitivity analysis was performed for the area weighted average curve number parameter, because a limitation to the CN method is that it is very sensitive to the curve number used when estimating runoff. The rural scenario area weighted average curve number was decreased by 5 and the urban scenario area weighted average curve number was increased by 5. The average difference in runoff from the storms in Table 7 was recalculated with rural area weighted average of 51.59 and an urban area weighted average of 74.27. Recharge for the CN sensitivity analysis was calculated in the same way described in section 4.6.1 (see Table 8b) and a used to develop another piecewise cubic interpolation function (Figure 16). Groundwater flux to the wetland was computed and compared to the groundwater flux computed in the urban scenario.

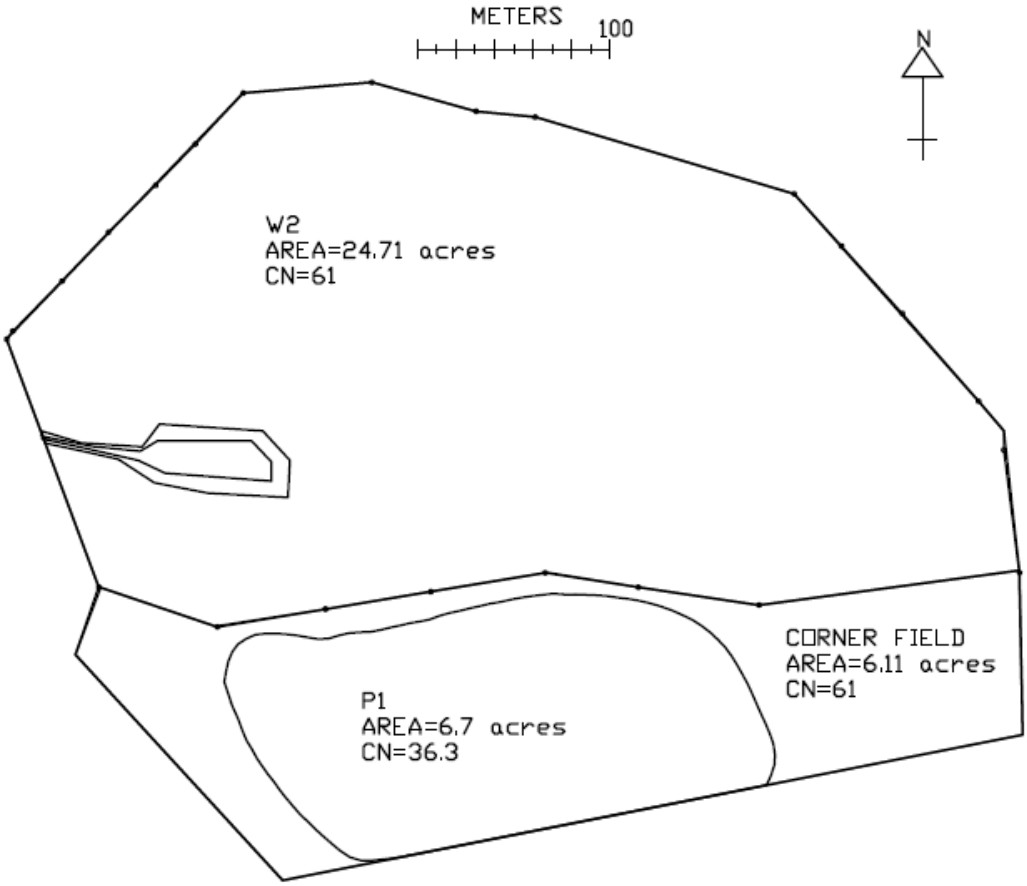

Figure 14: The watershed's current land use configuration (the rural scenario).

Table 5: Curve numbers for individual areas and the area weighted average curve number for the rural scenario

Lot	Area (ha)	Curve Number	Area Weighted Average CN
P1	2.71	36.3	56.59
W2	10.0	61	
Corner Field	2.47	61	

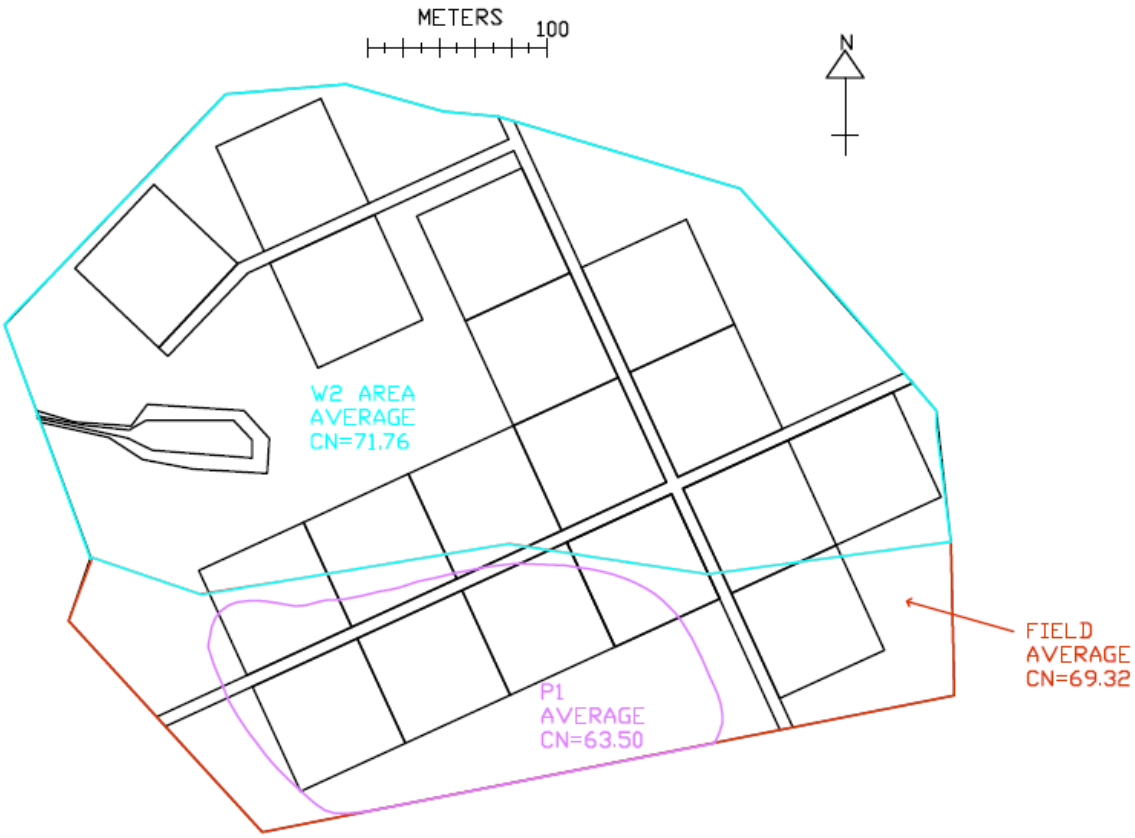

Figure 15: Plan for the urbanized watershed. The black squares are one acre lots.

Table 6: Curve numbers for individual areas and the area weighted aver curve number for the urban scenario

Urban Scenario W2 Parameters		
W2 Area (ac)	Field	13.32
	Lots	11.92
	Streets	1.26
Curve Number	Field	61
	Lots	81
	Streets	98
Area Weighted Average CN	Field+Lots+Streets	71.76
Urban Scenario Corner Field Parameters		
W2 Area (ac)	Field	3.59
	Lots	1.87
	Streets	0.28
Curve Number	Field	61
	Lots	81
	Streets	98
Area Weighted Average CN	Field+Lots+Streets	69.32
Urban Scenario P1 Parameters		
W2 Area (ac)	Field	2.88
	Lots	3.9
	Streets	0.292
Curve Number	Field	36.3
	Lots	81
	Streets	98
Area Weighted Average CN	Field+Lots+Streets	63.5
Area Weighted Average CN for the Entire Watershed		
69.92		

Table 7: A summary of the runoff differences for the rural and urban scenarios. Relative percent difference is calculated by $\frac{\alpha-\beta}{\alpha}\times 100$.

		Runoff Depth (mm/day)			
Return Period	Rainfall Depth (mm)	Rural (α)	Urban (β)	Difference	Relative Percent Difference
1yr-24hr	82.55	7.9502	26.162	-18.2118	-229.07
2yr-24hr	101.6	15.24	39.2684	-24.0284	-157.67
5yr-24hr	119.38	23.495	52.5526	-29.0576	-123.68
10yr-24hr	139.7	34.3154	68.6562	-34.3408	-100.07
25yr-24hr	165.1	49.5554	089.789	-40.2336	-81.19
50yr-24hr	186.69	63.7032	108.4072	-44.704	-70.18
100yr-24hr	193.04	68.0212	113.9698	-45.9486	-67.55
Mar-07	80.01	7.1374	24.511	-17.3736	-243.42
Average Runoff Difference				-31.7373	
Average Runoff Difference/300 days				105.791	

Table 8a: Parameter summary statistics for the sensitivity analysis. Hydraulic conductivity values taken from Overbaugh (1996), Appendix B; Potential evapotranspiration values taken from Hoogenboom (2009); Recharge values derived from baseflow analysis of Murder Creek discharge hydrograph for the month of September in the years 2002 through 2006 (Anonymous, 2002-2006); Specific yield values taken from Dunne and Leopold (1978), pg 201.

Parameter	K (mm/day)	PET (mm/day)	Recharge (mm/day)	Specific yield (-)
Mean	281.16979	2.977083	6.75E-02	0.255
Median	271.3304	2.974	5.47E-02	0.255
Standard Deviation	31.500443	0.523813	6.36E-02	0.14577
Range	95.2282	1.964667	0.149649	0.49
Minimum	249.8365	2.182	4.47E-03	0.01
Maximum	345.0647	4.146667	0.154124	0.5
Count	10	12	5	50

Table 8b: A summary of runoff for the curve number (CN) sensitivity analysis. Relative percent difference is calculated by $\frac{\alpha-\beta}{\alpha}\times 100$.

		Runoff Depth (mm/day)			
Return Period	Rainfall Depth (mm)	Rural (α)	Urban (β)	Difference	Relative Percent Difference
1yr-24hr	82.55	4.445	33.7058	-29.2608	-658.29
2yr-24hr	101.6	9.9568	48.4378	-38.481	-386.48
5yr-24hr	119.38	16.5862	63.0428	-46.4566	-280.09
10yr-24hr	139.7	25.6286	80.4418	-54.8132	-213.88
25yr-24hr	165.1	38.7604	102.9208	-64.1604	-165.53
50yr-24hr	186.69	51.2064	122.5296	-71.3232	-139.29
100yr-24hr	193.04	55.0672	128.3462	-73.279	-133.07
Mar-07	80.01	3.8608	31.8262	-27.9654	-724.34
Average Runoff Difference				53.967743	
Average Runoff Difference/300 days				0.179892	

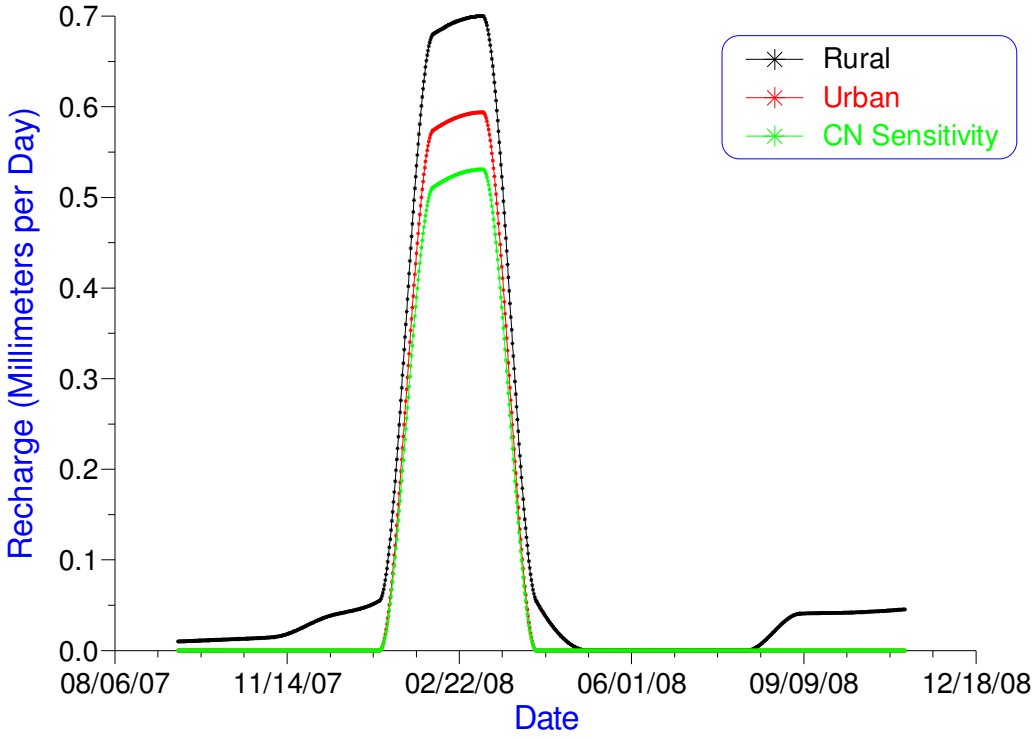

Figure 16: The piecewise cubic interpolation functions of recharge for the rural scenario, urban scenario, and the curve number (CN) sensitivity test.

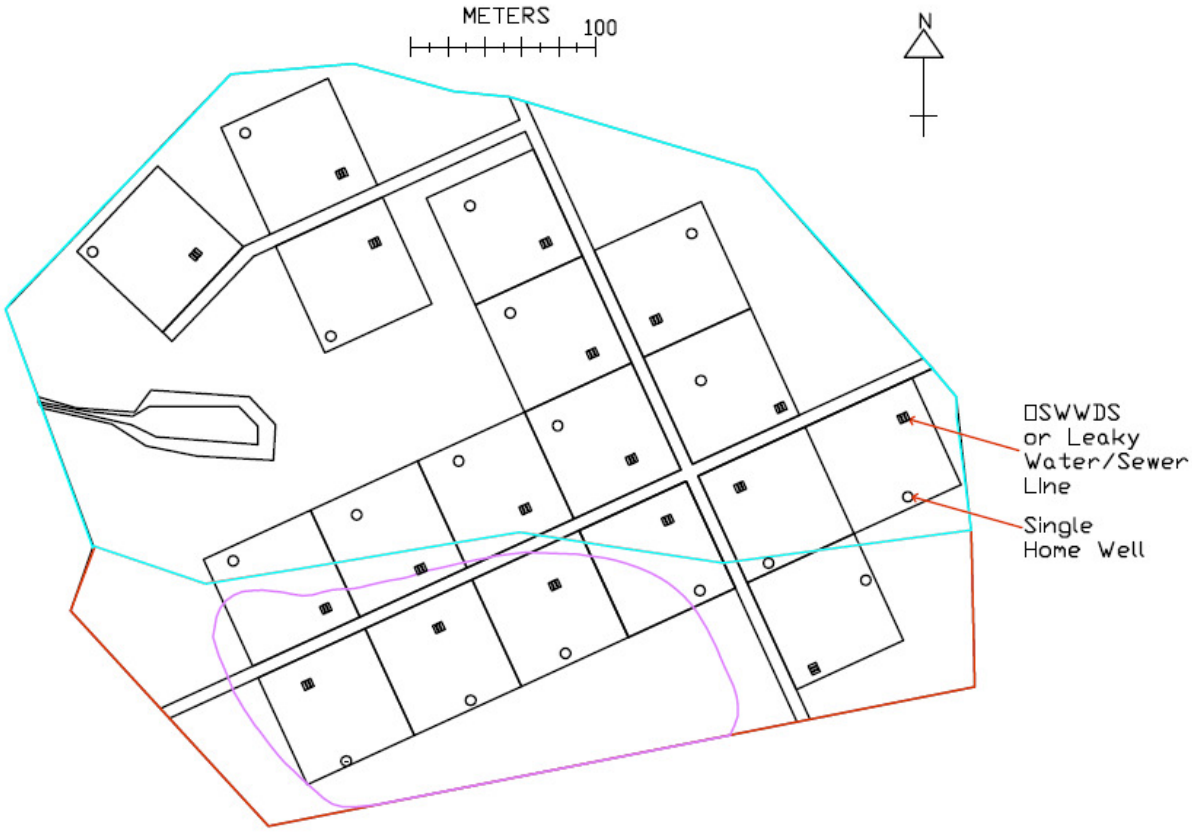

Figure 17: Locations of wells (open circles) and onsite wastewater disposal systems or leaky water/sewer lines (black squares) in the domain.

Chapter 5: Mathematical Statement

The assumptions used to describe the physics of groundwater movement in an unconfined aquifer are discussed in this chapter. Further assumptions are described that reduce the problem to one that is suited to computer modeling and a description of the computer model, Comsol, is provided.

5.1 Governing Equation

For the most general case, the equation for time dependent groundwater flow in a heterogeneous isotropic aquifer can be written

$$\frac{\partial}{\partial x}\left(K\frac{\partial h}{\partial x}\right)+\frac{\partial}{\partial y}\left(K\frac{\partial h}{\partial y}\right)+\frac{\partial}{\partial z}\left(K\frac{\partial h}{\partial z}\right)+R=S\frac{\partial h}{\partial t} \qquad (5.1)$$

Where:

K is hydraulic conductivity (L/t)

h is hydraulic head (L)

R represents sources and sinks (L/t)

S is the storage of the aquifer (unitless)

In this form, gains and losses of fluid mass are accounted for in the storage term. The dimensionality of Equation 5.1 can be reduced by one dimension by taking the hydraulic approach where, in the broadest application, a three dimensional domain is subdivided into its constituents: Aquifers, aquitards, and aquicludes. Inherent in this approach is the assumption that flow in an aquifer is essentially horizontal to an impervious base.

$$\frac{\partial}{\partial x}\left(Kh\frac{\partial h}{\partial x}\right)+\frac{\partial}{\partial y}\left(Kh\frac{\partial h}{\partial y}\right)+R=S_y\frac{\partial h}{\partial t} \qquad (5.2)$$

Equation 5.2 is the equation for flow groundwater flow in an unconfined aquifer where the specific yield, S_y, is the unitless product of the aquifer thickness, b, and the storage, S. Bear (1972) defines specific yield as the amount of water saturated media will yield by gravity drainage (volume of water produced per unit aquifer area per unit decline in head). An analytical solution to Equation 5.2 does not exist because it is non-linear because head, h, and the derivative of head must be known. However, two methods exist to linearize equation 5.2 and circumvent the problem of solving a non-linear differential equation. By acknowledging that

$$\frac{\partial h^2}{\partial x} = 2h\frac{\partial h}{\partial x} \qquad (5.3)$$

$$\frac{\partial h^2}{\partial y} = 2h\frac{\partial h}{\partial y} \qquad (5.4)$$

Equation 5.2 can be rewritten

$$\frac{\partial}{\partial x}\left(K\frac{\partial h^2}{\partial x}\right)+\frac{\partial}{\partial y}\left(K\frac{\partial h^2}{\partial y}\right)+2R = 2S_y\frac{\partial h}{\partial t} \qquad (5.5)$$

Another, simpler, technique was used to linearize this problem. The product of hydraulic conductivity K and the known aquifer saturated thickness, b, is transmissivity, T, which has units of L^2t^{-1}.

$$\frac{\partial}{\partial x}\left(T\frac{\partial h}{\partial x}\right)+\frac{\partial}{\partial y}\left(T\frac{\partial h}{\partial y}\right)+R = S_y\frac{\partial h}{\partial t} \qquad (5.6)$$

Equation 5.6 invokes the Dupuit assumptions that equipotentials are horizontal and that flow is strictly horizontal.

The solution for groundwater flow over sloping beds is a classic groundwater modeling problem. Kalaidzidou-Paikou and Karamouzis (1995) note that incorporation of a basis to change the direction of the gravity vector in K can give a better approximation to the solution of

groundwater flow over sloping beds than equation 5.6. Equation 5.6, modified to incorporate flow parallel to an impervious base, can be restated as:

$$\frac{\partial}{\partial x}\left(T\cos^2\alpha_x\frac{\partial h}{\partial x}\right)+\frac{\partial}{\partial y}\left(T\cos^2\alpha_y\frac{\partial h}{\partial y}\right)+R=S_y\frac{\partial h}{\partial t} \qquad (5.7)$$

Where:

α_x is the angle of the impervious base relative to some datum in the x direction

α_y is the angle of the impervious base relative to some datum in the y direction

5.2 Description of the Computer Model Comsol

Comsol is a commercial finite element analysis, simulation, and visualization software. Comsol has various integrated utilities, such as automatic mesh generation and refinement, as well as a rudimentary Computer Aided Drafting (CAD) utility. Comsol has built in partial differential equation modules designed for certain physics and engineering problems, including problems that involve coupled phenomena, heterogeneous and anisotropic materials, and time dependent problems. Due to availability, Comsol's time dependent convection diffusion model was used. The convection diffusion model was chosen because it was the most easily adaptable to a groundwater problem. Equations 5.8 through 5.12 show the progression of changes made to the original governing equation in the Comsol convection diffusion model to fit a groundwater modeling application.

The governing equation in Comsol's predefined convection diffusion module is:

$$\delta_{ts}\frac{\partial c}{\partial t}+\nabla\cdot(-D\nabla c)=R-\mathbf{u}\cdot\nabla c \qquad (5.8)$$

Where:

δ_{ts} is a time scaling coefficient that can be substituted for S_y

c is the state variable concentration that can be substituted for h

t is time

D is the diffusion coefficient that can be substituted for T

R is the reaction rate that can be substituted for recharge

u is the convective velocity in a particular direction

By expanding equation 5.8 and setting the convective velocity term (**u)** to zero equation 5.8 becomes:

$$\delta_{ts}\frac{\partial c}{\partial t}+\frac{\partial}{\partial x}\left(-D\frac{\partial c}{\partial x}\right)+\frac{\partial}{\partial y}\left(-D\frac{\partial c}{\partial y}\right)=R \qquad (5.9)$$

Rearranging equation 5.9 and expressing D as:

$$D=Kb\cos^2\alpha_i=T\cos^2\alpha_i \qquad (5.10)$$

Where:

K is hydraulic conductivity (L/t)

b is the average saturated thickness of the aquifer (L)

$\cos^2\alpha_i$ is the slope of the impervious base in the x or y direction (radians)

T is the aquifer transmissivity (L^2/t)

Equation 5.9 becomes:

$$\frac{\partial}{\partial x}\left(T\cos^2\alpha_x\frac{\partial c}{\partial x}\right)+\frac{\partial}{\partial y}\left(T\cos^2\alpha_y\frac{\partial c}{\partial y}\right)+R=\delta_{ts}\frac{\partial c}{\partial t} \qquad (5.11)$$

Finally, by asserting that c is equal to h, and replacing the time scaling coefficient (δ_{ts}) with specific yield (S_y) yields:

$$\frac{\partial}{\partial x}\left(T\cos^2\alpha_x\frac{\partial h}{\partial x}\right)+\frac{\partial}{\partial y}\left(T\cos^2\alpha_y\frac{\partial h}{\partial y}\right)+R=S_y\frac{\partial h}{\partial t} \qquad (5.12)$$

This is identical to the governing equation (equation 5.7).

5.3 Heterogeneity

If the permeability of a geologic formation does not vary with space, the formation is homogeneous. Most groundwater modeling codes handle the heterogeneous case, and can thereby handle the homogeneous case as well, by treating K as a function of space, K = f(x,y). Comsol can handle the heterogeneous case several ways, one of which is, by creating a rectangular gridded linear interpolation function that "lay" over the domain. The coordinates of the four corners of the grid and the values of a hydraulic conductivity were specified at the coordinates of the grid and interpolated across the grid.

5.4 Boundary Conditions

For an initial value problem to be well posed appropriate boundary conditions and initial conditions must be assigned to the domain. This thesis used two types of boundary conditions: Dirichlet and Neumann.

Dirichlet boundary conditions are boundaries of prescribed head. Stated mathematically:

$$h = f(x, y) \; on \; S \qquad (5.13)$$

where S is the boundary. A special case for Dirichlet boundaries exists when h is constant for all locations on S. Dirichlet boundaries were used on the thalweg of the wetland and stream to represent the height of the watertable there.

Neumann boundary conditions are boundaries of prescribed flux. Stated mathematically:

$$q_n = f(x, y) \; on \; S \qquad (5.14)$$

where q_n is the outward normal flux. The special case for Neumann is the no flow boundary, mathematically written as

$$q_n = 0 \qquad (5.15)$$

The no flow boundaries were applied at the ridges of the site because ridges are groundwater divides. No flow boundaries were also applied to flow lines at the western edge of the domain, because flow lines do not cross.

Internal continuity boundaries are special Neumann boundaries inside the domain where flux is specified for the upward and downward sides of the boundary. The flux that reaches the upward side of the boundary is set equal to the flux on the downward side of the boundary. Mathematically stated, a continuity boundary takes the form

$$\mathbf{n} \cdot (q_1 - q_2) = 0 \qquad (5.16)$$

Where

n is the unit vector normal to the boundary

Continuity boundaries were used to describe the geometry of the wetland.

Chapter 6: Results

6.1 Field Observations

Spring flow was collected on a continuous basis from January 1, 2007, to November 7, 2008. In total, the spring flowed for 34 days during September 10, 2007, through November 3, 2008. In general, the spring flows the most during the recharge months when ET is at a low (late fall through late winter) and flows the least during the months when ET is at a high (late winter to late fall). The spring stopped flowing around March 7, 2007, the first time the spring ever stopped flowing since monitoring started with a flume in 1999. The spring began to flow again in November 2007 for a very short period of time (which coincides with a drop in evapotranspiration during the colder months), stopped shortly after, began to flow again on January 1, 2008, and stopped flowing again around March 2008. The spring did not flow again during the period of observation.

Rainfall (mm) was collected on a continuous basis from January 1, 2007 to November 7, 2008 as well. Rainfall and cumulative rainfall are shown in Figure 18. In the southeast, groundwater recharge occurs in the cooler months, when little rainfall is being evapotranspired by vegetation, typically mid to late September through late March or early April. Table 9 compares total monthly rainfall for September 2007 through October 2008 to the long term average rainfall for those months. Every month during that time period, except December 2007 and October 2008, the total monthly rainfall is less than the long term average. There is also a rainfall deficit for seven of the nine months when recharge normally occurs.

Head (meters above sea level (m asl)) was collected on a continuous basis from September 5, 2007 to November 3, 2008 in wells EPA 2, EPA 5, and EPA 7 as shown in Figure 18. Data from EPA 3 is not shown in Figure 18 because there were problems with the pressure transducer in that well. Seasonal recharge is evident from the peaks and valleys of the data.

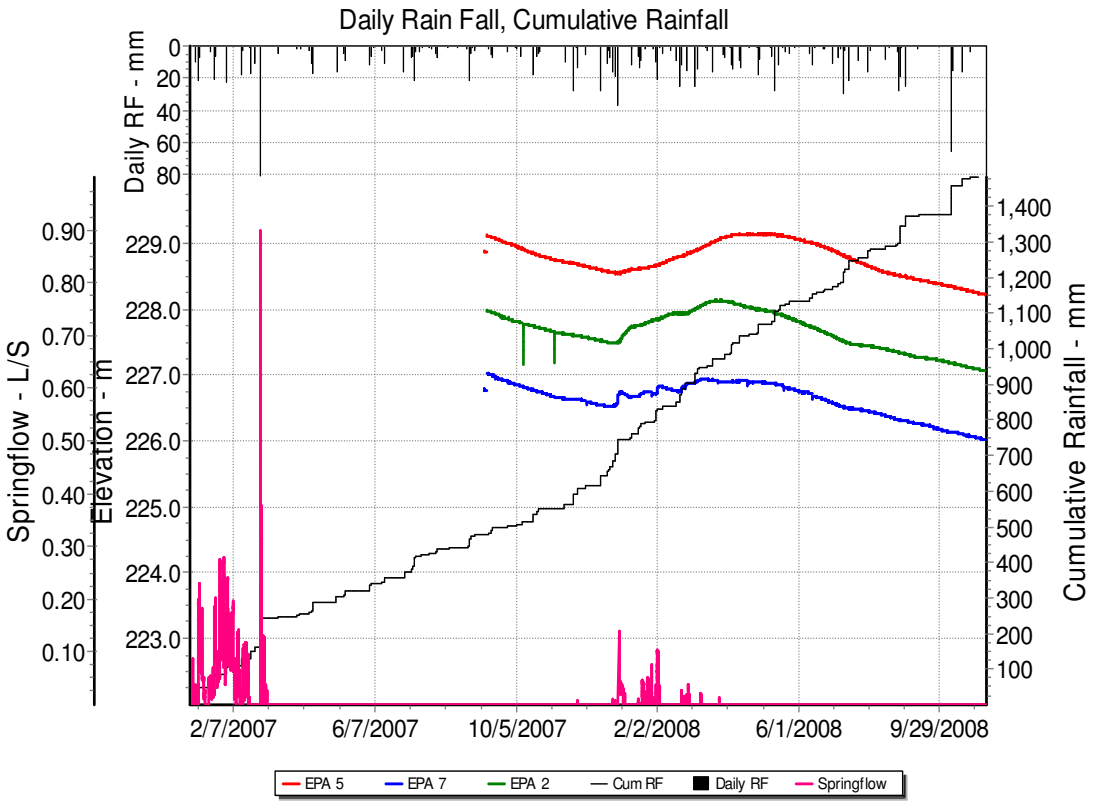

Figure 18: All data collected in the vicinity of W2 from January 1, 2007, to November 3, 2008.

Table 9: Relative difference between total rainfall by month and the long term average rainfall for Sept-2007 through Oct-2008. The negative sign indicates that there was a rainfall deficit. Relative difference is defined as $\frac{\alpha - \beta}{\alpha} \times 100$.

Month-Year	Total Rainfall (mm) (β)	Long Term Average (mm) (α)	Relative Difference
Sept-07	23.52	86.73	72.88
Oct-07	60.515	75.46	19.81
Nov-07	50.225	86.73	42.09
Dec-07	108.535	100.94	-7.52
Jan-08	63.945	111.965	42.89
Feb-08	96.53	110.985	13.02
Mar-08	79.135	130.83	39.51
April-08	89.915	94.815	5.17
May-08	75.46	91.385	17.43
June-08	48.02	98	51.00
July-08	88.2	116.865	24.53
Aug-08	85.75	91.875	6.67
Sept-08	3.43	86.73	96.05
Oct-08	109.515	75.46	-45.13

6.2 Modeling Results

6.2.1 Steady-state and Transient Calibration Results

The model was calibrated to steady-state after 236 runs using trial and error. Heads observed at wells EPA 2, EPA 3, and EPA 7 were within the specified tolerance of 0.1 meters. Figure 19 displays the contoured head distribution of the steady-state solution with flow lines. The steady-state solution was the initial condition for the transient model. The transient model was calibrated by adjusting the rate of recharge to match the shape of the EPA 2 and EPA 7 well hydrographs from September 10, 2007 to November 3, 2008. Figure 20 and Figure 21 display the calibrated well hydrographs for wells EPA 2 and EPA 7, respectively. Figure 22 and Figure 23 display the recharge and the PET model inputs, respectively.

6.2.2 Development Scenarios Results

Flux across the constant head boundaries were calculated in the rural, urban, leaky urban, septic, and septic well scenarios. On average, the relative difference between the rural scenario flux and the urban scenario flux was 1.5%. The relative difference between the rural and the leaky urban scenario was 13.2%. The relative difference between the rural scenario and the septic scenario was 27.0%. The relative difference between the septic well and rural scenario was 1.4%. The relative difference between the urban and septic scenarios was 29.0%. The relative difference between the urban scenario and the septic well scenario was 2.9 %. The relative difference between the urban scenario and the leaky urban scenario was 14.9%. Flux for every scenario is displayed in Figure 24. The model water budget for each scenario is summarized in Table 10, and relative flux differences are summarized in Table 11.

6.2.3 Comparison of Calculated and Inferred Advective Velocities

Advective velocity is defined as the Darcy velocity divided by the effective porosity and is the average linear velocity at which conservative solutes move within the pores of the aquifer material (Freeze and Cherry, 1979). The magnitude of the calculated advective velocity at a point near the spring was plotted in Figure 25 over the 423 day simulation to compare computed advective velocities to inferred advective velocity in Amirtharajah *et al.* (2002). The highest calculated advective velocity was 0.42 m/d and the inferred advective velocity was 0.65 m/d.

6.2.4 Sensitivity Analysis Results

The sensitivity analysis took place over 12 model runs for five different model parameters. Transmissivity, PET, recharge and specific yield were changed individually by ±two standard deviations. Changes in head at the locations of wells EPA 2, EPA 3, and EPA 7 are displayed in Figure 26. Changes in groundwater flux to the wetland were recorded and displayed in Figure 27. In addition, the hydraulic conductivity function was rotated 90° three times (Figure 28) and changes in residual head and changes in groundwater flux to the wetland were recorded in Figure 29 and Figure 30, respectively. Changes in head with changes in specific yield were evaluated over the entire 423 day simulation. Heads were recorded at wells EPA 2 and EPA 7 and plotted in Figure 31 and Figure 32, respectively. Changes in groundwater flux were also recorded and plotted in Figure 33.

The groundwater flux sensitivity to a broader range of curve numbers between the rural and urban scenarios was evaluated. The groundwater flux response to a broader range of curve numbers for the urban and rural scenario is displayed in Figure 34. The sensitivity test results are summarized in Tables 12a through 12c.

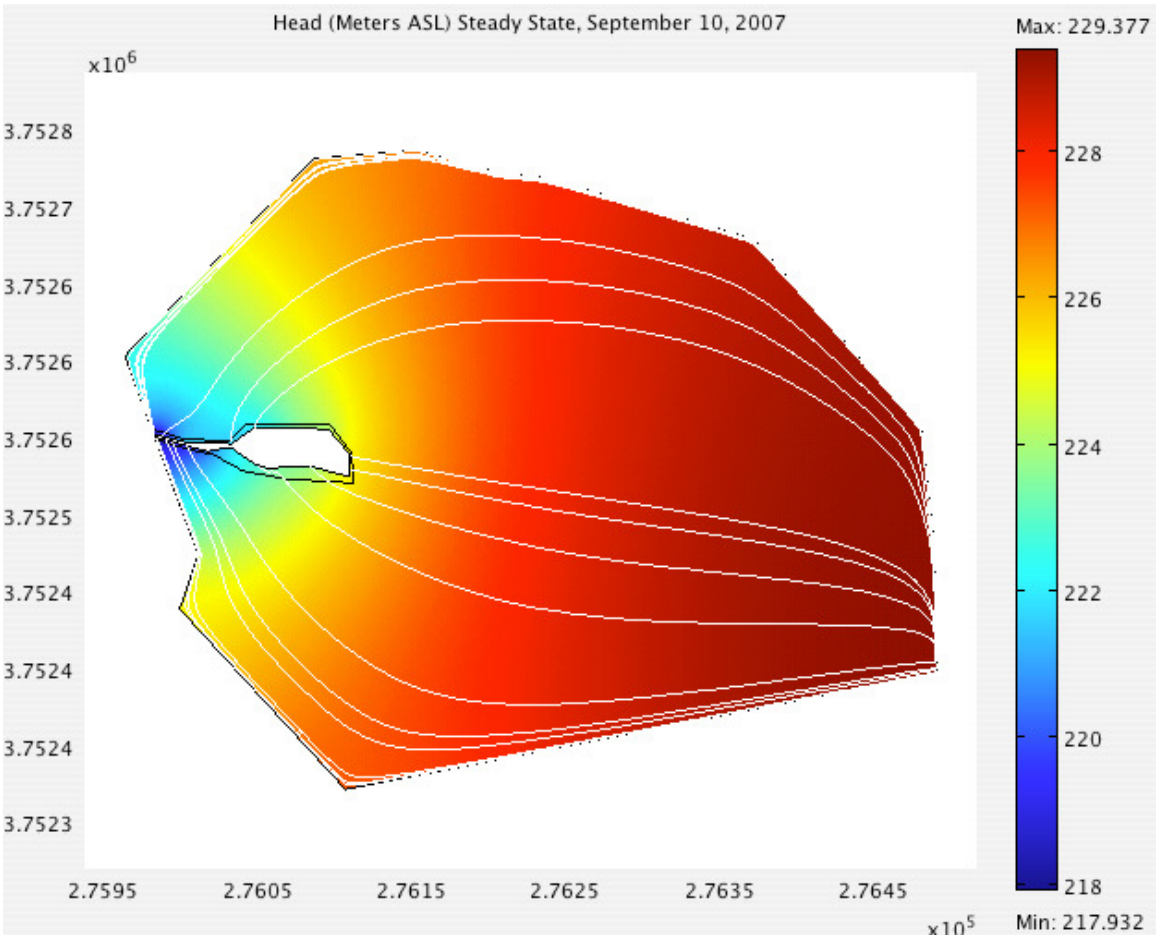

Figure 19: Steady-state watertable configuration. The white lines are streamlines.

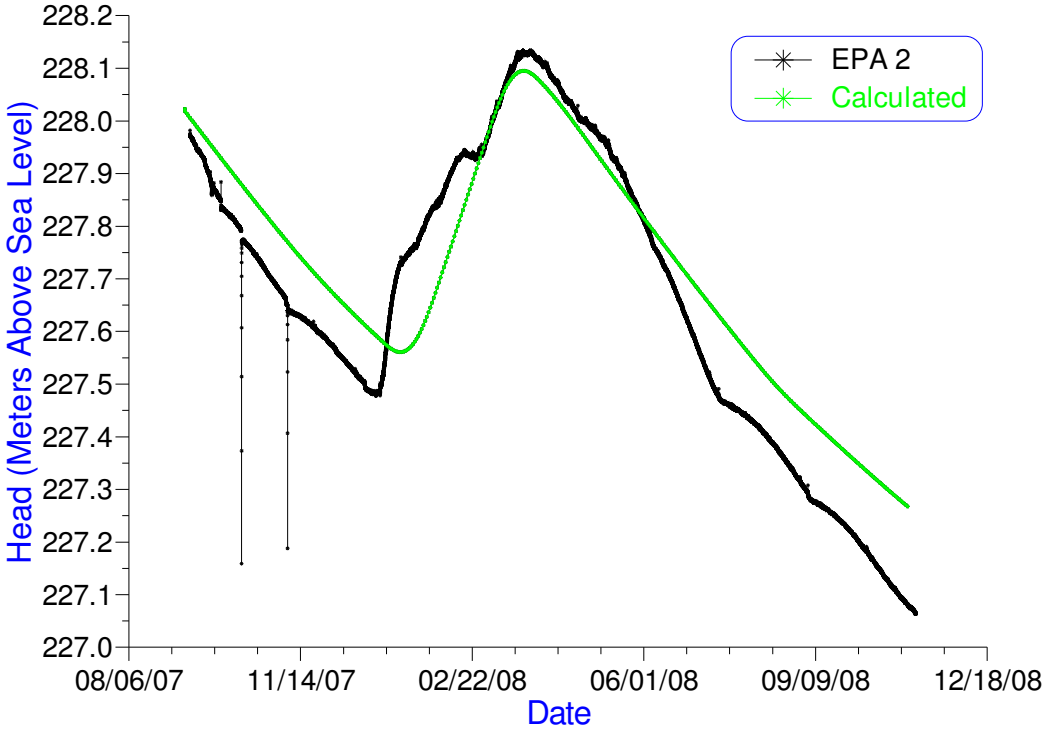

Figure 20: Observed and model calculated heads at well EPA 2.

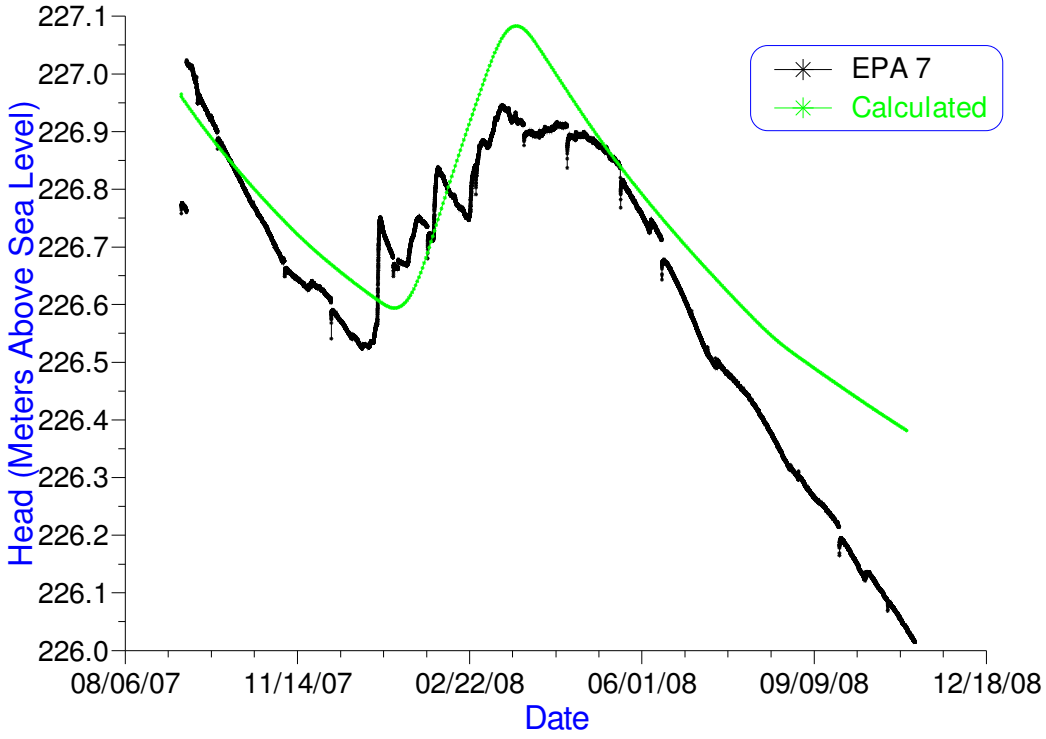

Figure 21: Observed and model calculated heads at well EPA 7

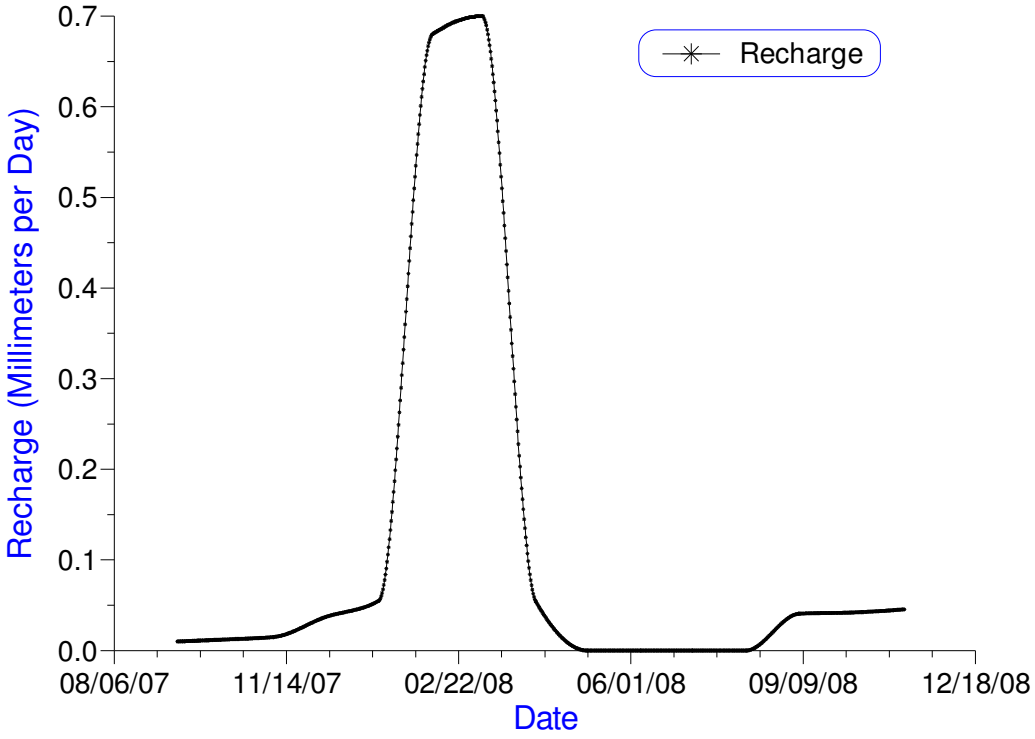

Figure 22: Plot of recharge used for the calibrated transient solution. The shape of the recharge function is based on the seasonal groundwater recharge typical of the southeast United States.

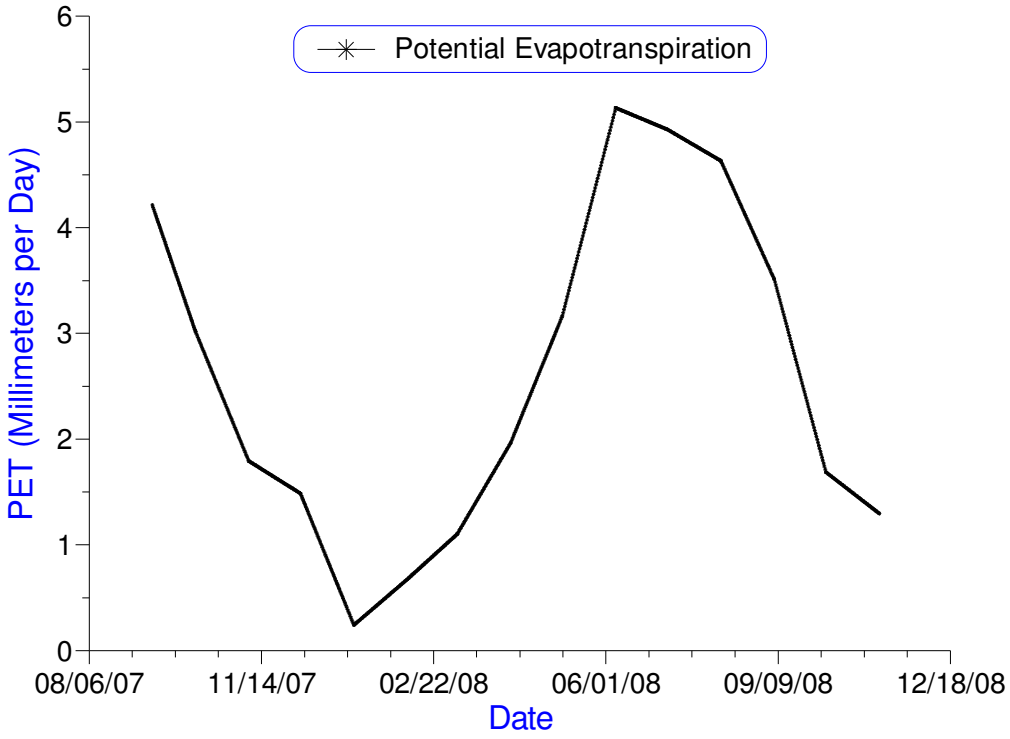

Figure 23: Piecewise cubic interpolation function of potential evapotranspiration. The shape of the function is based on monthly temperature variations.

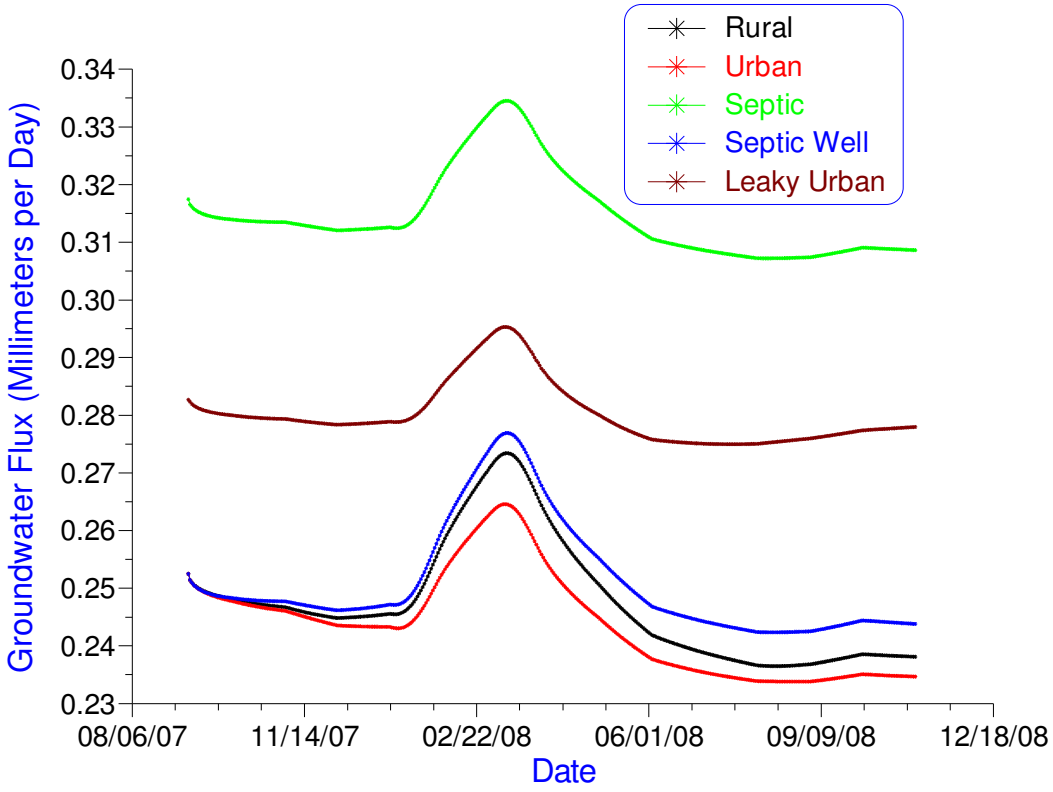

Figure 24: Groundwater flux to the wetland for each scenario. The area of the watershed is 1.58E5 m^2. Flux is reported in (mm^3/day)/watershed area (mm^2).

Table 10: Water budgets for each scenario. The values for each component of the budget are averages for the 423 day simulation. The value of each component is presented in terms of Flux (mm^3)/watershed area (mm^2). The superscripts denote the area over which a volume of water was applied, or the baseflow contributing area.

Scenario	Recharge[a] (mm/day)	PET[b] (mm/day)	Q_{septic}[c] (mm/day)	Q_{wells}[a] (mm/day)	$Q_{sewer/water}$[c] (mm/day)	$Q_{wetland}$[a] (mm/day)
Rural	0.12	2.58	0.00	0.00	0.00	0.25
Urban	0.08	2.58	0.00	0.00	0.00	0.25
Leaky Urban	0.08	2.58	0.00	0.00	11.00	0.28
Septic	0.08	2.58	450.00	0.00	0.00	0.32
Septic-well	0.08	2.58	450.00	-0.13	0.00	0.25

[a]Watershed area: 1.58E5 m^2

[b]Wetland torus area: 1091.65 m^2

[c]Leaky water/sewer pipes or septic leach field area: 25.28 m^2

Table 11: Average relative flux differences for each scenario. Relative difference is defined as $\frac{\alpha - \beta}{\alpha}$.

Scenario Comparison (α-β)	Relative Flux Difference (mm/d)	Flux Percent Difference
Rural-Urban	0.015	1.5
Rural-Leaky Urban	-0.132	-13.2
Rural-Septic	-0.270	-27.0
Rural-Septic Well	-0.014	-1.4
Urban-Septic	-0.29	-29.0
Urban-Septic Well	-0.029	-2.9
Urban-Leaky Urban	-0.149	-14.9

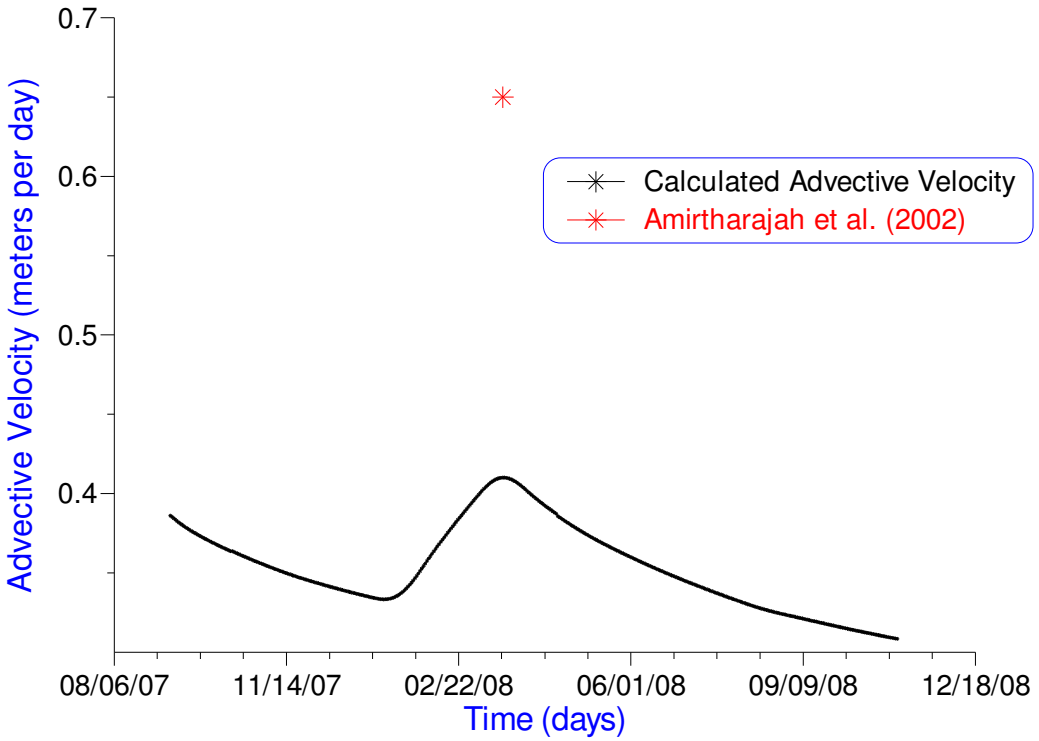

Figure 25: Calculated magnitude of the advective velocity at a point near the spring using an effective porosity of 0.05.

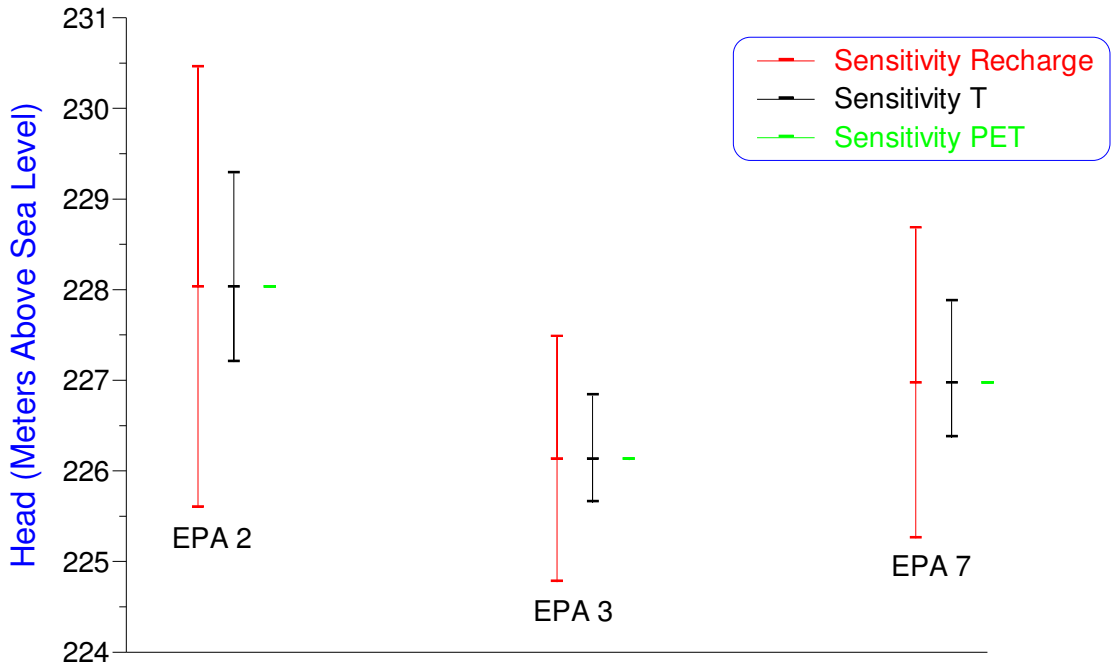

Figure 26: Sensitivity of steady-state solution to changes in recharge, transmissivity (T), and potential evapotranspiration (PET).

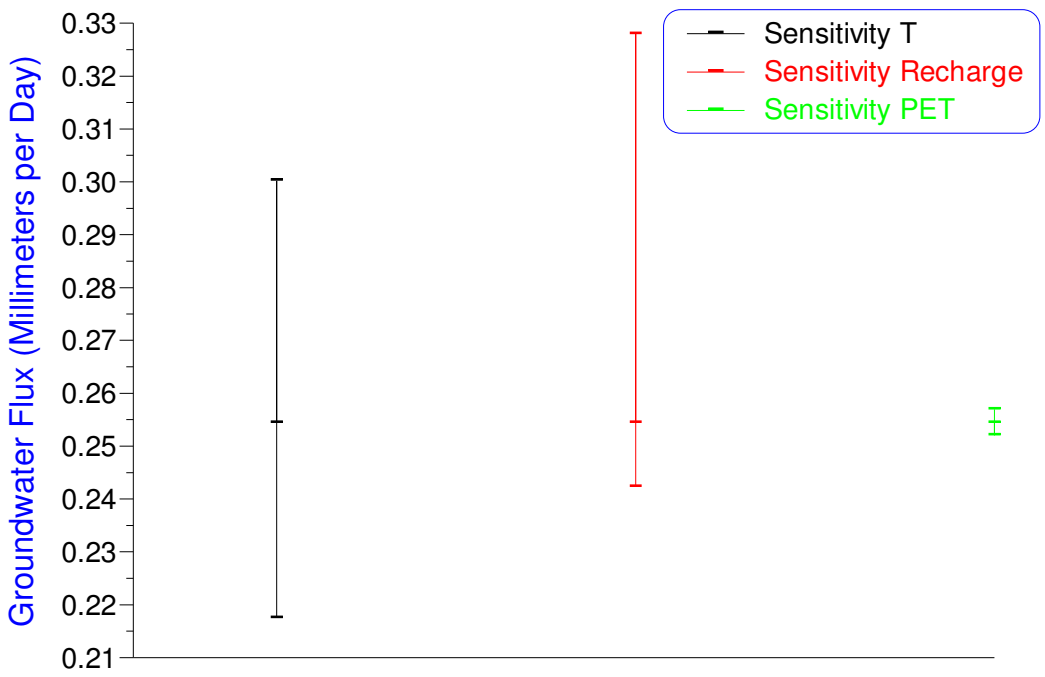

Figure 27: Sensitivity of computed groundwater flux to changes in recharge, transmissivity (T), and potential evapotranspiration (PET).

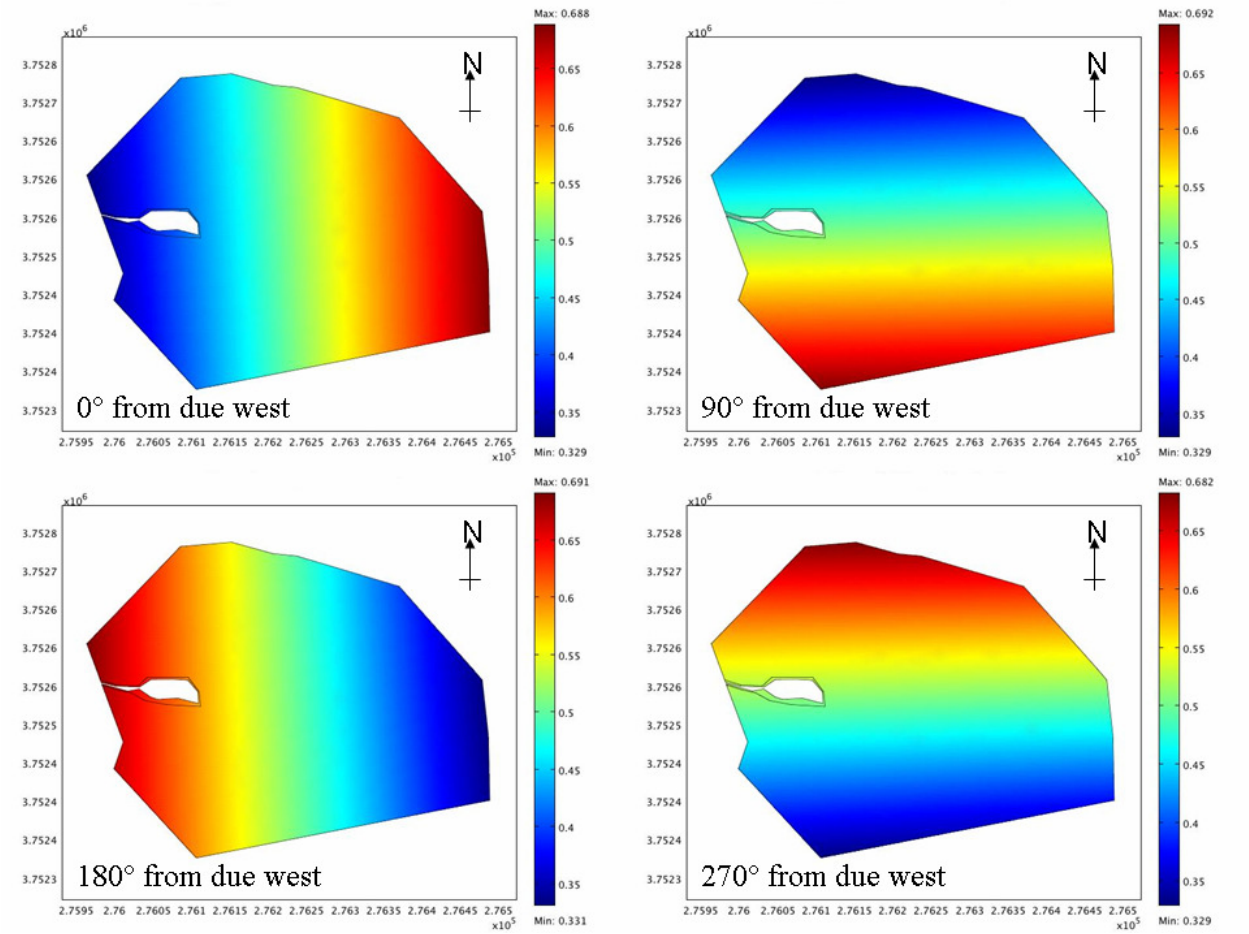

Figure 28: Plot of hydraulic conductivity interpolation function as the function is rotated 360° in 90° increments. The red and blue shaded regions represent the maximum and minimum values of hydraulic conductivity, respectively.

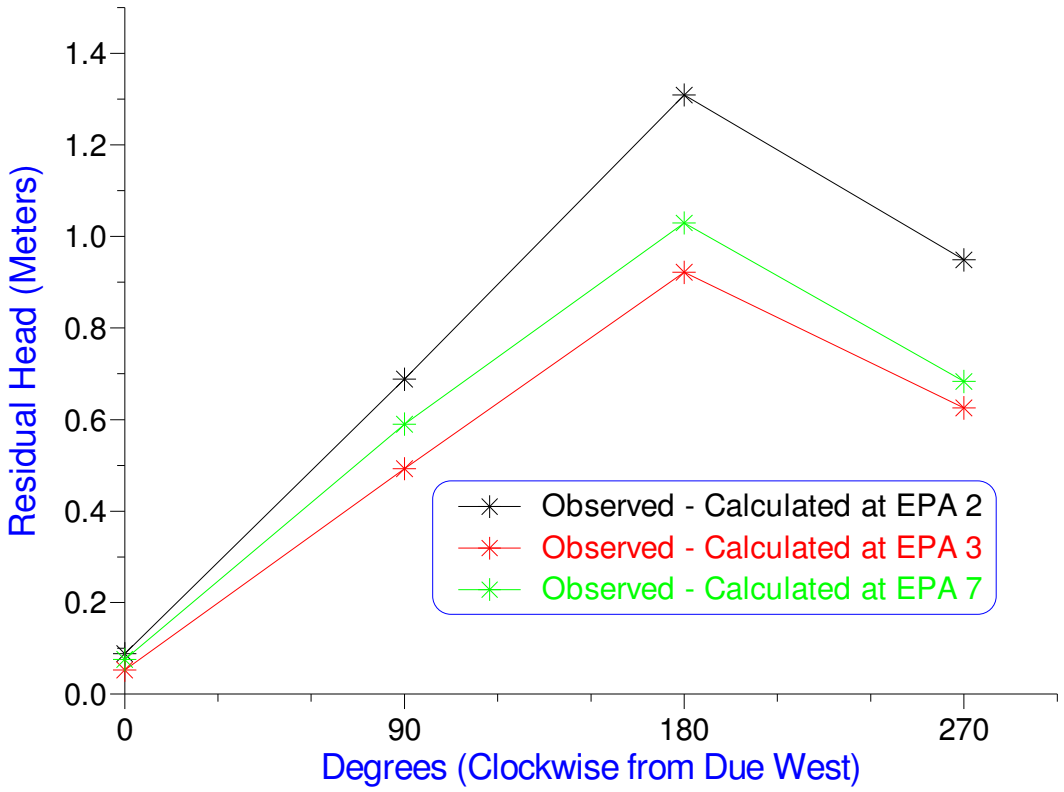

Figure 29: Residual head calculated from rotation of transmissivity (via the rotation of the hydraulic conductivity interpolation function). Residual head is observed head minus calculated head.

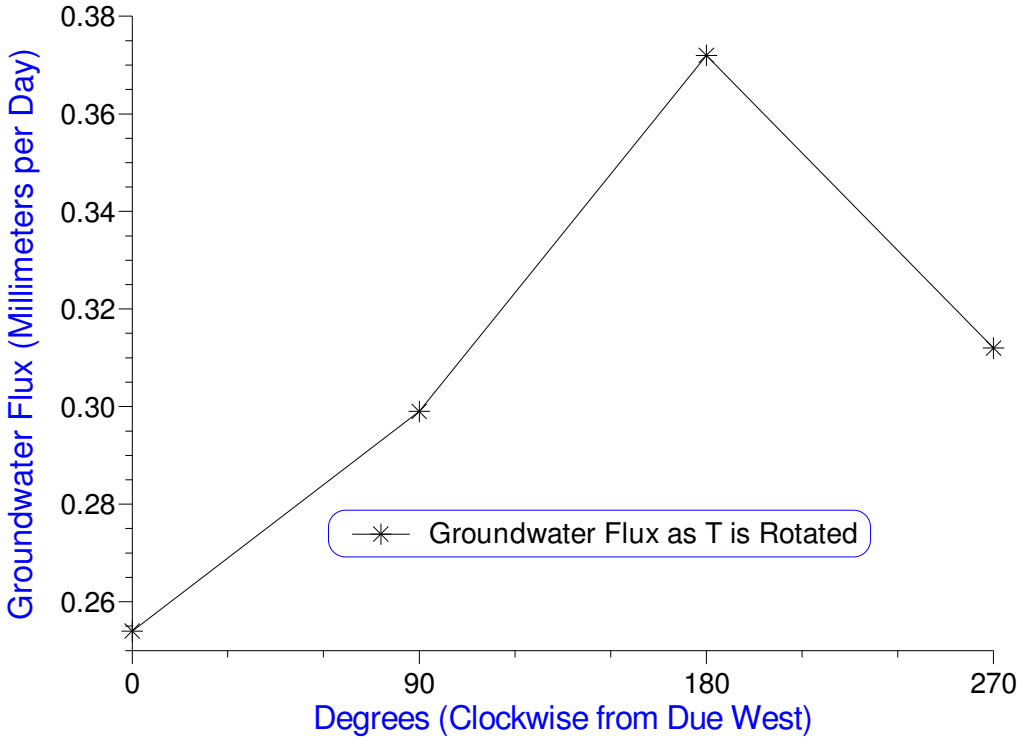

Figure 30: Groundwater flux sensitivity to the rotation of transmissivity.

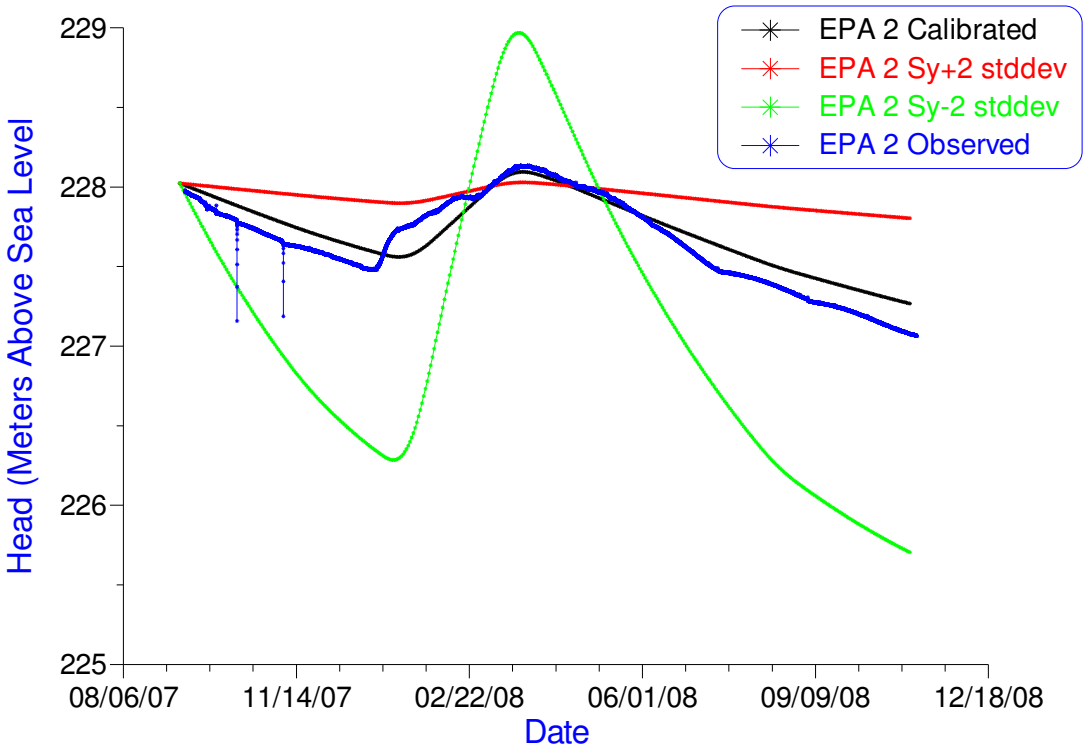

Figure 31: Sensitivity of transient solution to changes in specific yield at EPA 2.

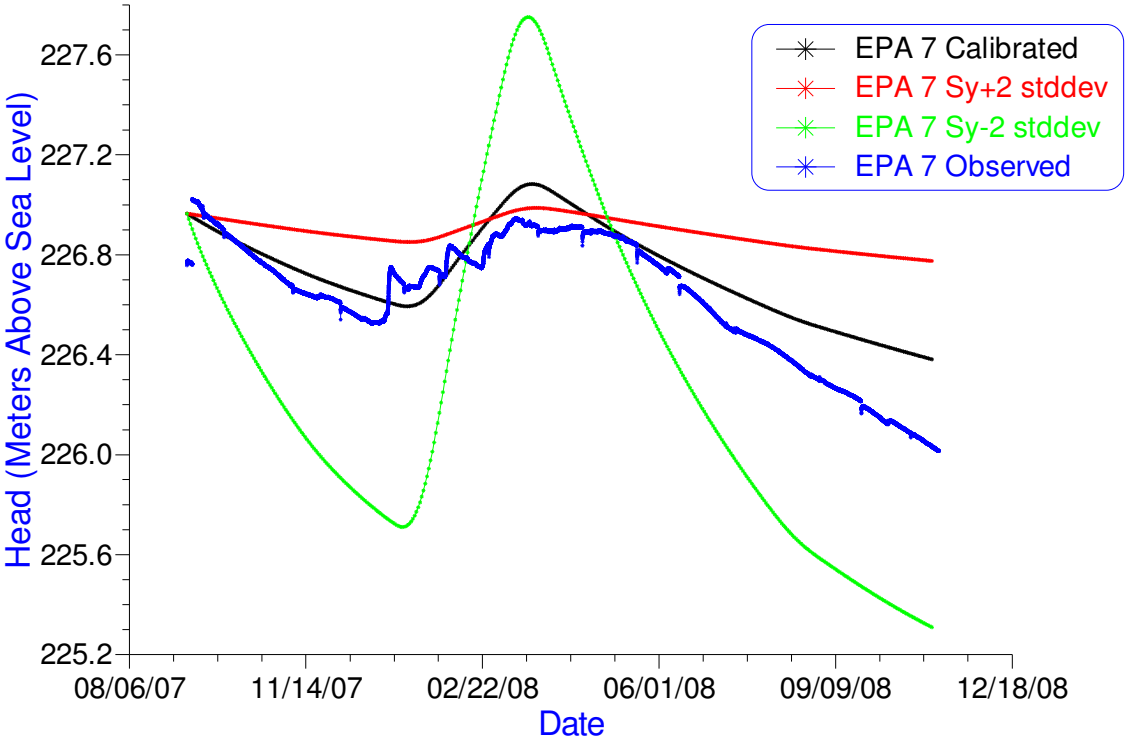

Figure 32: Sensitivity of transient solution to changes in specific yield at EPA 7.

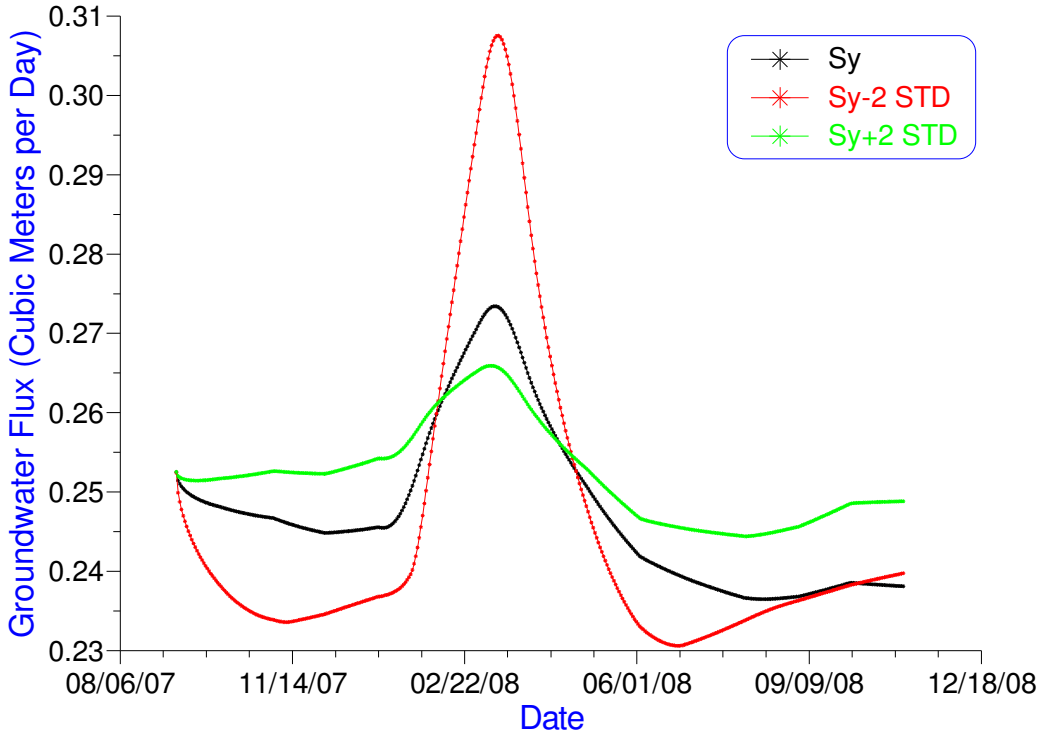

Figure 33: Sensitivity of calculated groundwater flux to changes in specific yield.

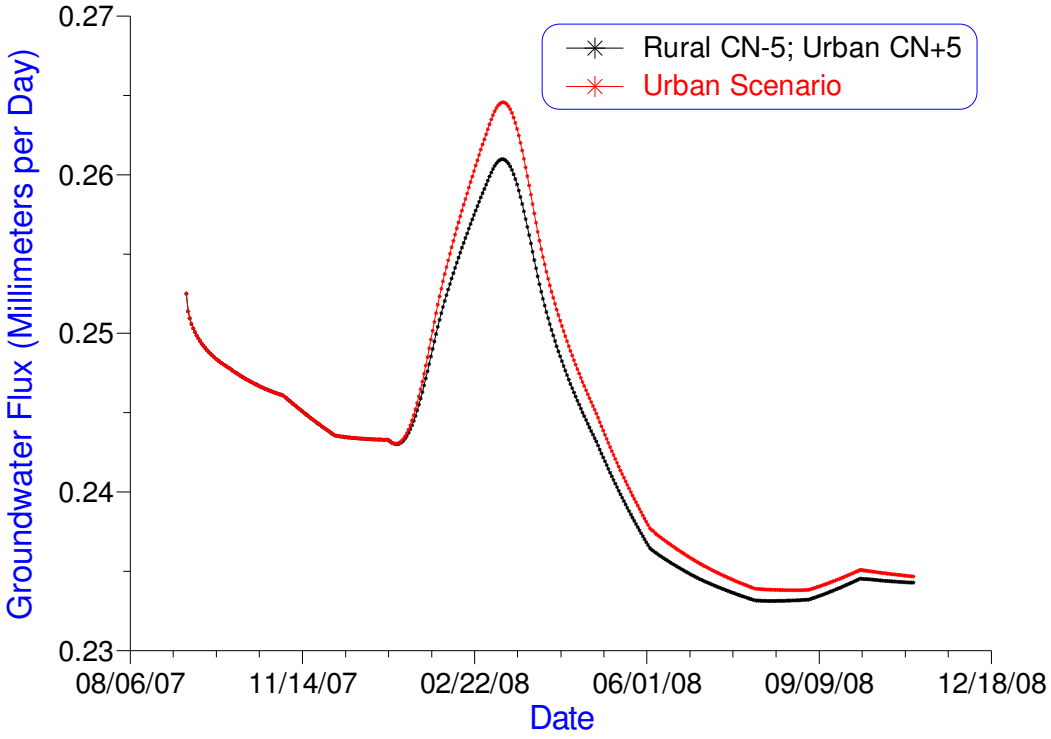

Figure 34: Calculated flux to the wetland in the urban scenario and the curve number (CN) sensitivity analysis.

Table 12a: Summary of ranges of head and groundwater flux from model sensitivity tests. T is transmissivity, PET is potential evapotranspiration, Sy is specific yield.

Head Response to Incremental Changes				
Difference from Calibrated Head (mm)				
Parameter		Calibrated	+2STD	-2STD
T	EPA 2	0.00	820.0	-1260.0
	EPA 3	0.00	470.0	-710.0
	EPA 7	0.00	590.0	-910.0
Recharge	EPA 2	0.00	-2430	2430.0
	EPA 3	0.00	-1350.0	1350.0
	EPA 7	0.00	-1710.0	1710.0
PET	EPA 2	0.00	0.00	0.00
	EPA 3	0.00	0.00	0.00
	EPA 7	0.00	0.00	0.00
S_y	EPA 2	0.00*	-680.0*	170.0*
	EPA 7	0.00*	-620.0*	440.0*
Baseflow Response to Incremental Changes				
	Parameter	Calibrated	+2STD	-2STD
Difference from Calibrated Flux (mm/day)	T	0.00	0.05	-0.04
	Recharge	0.00	0.07	-0.01
	PET	0.00	0.00	0.00
	Sy	0.00*	0.00*	0.00*

*Based on the average of the time series data

Table 12b: Summary of ranges of head and groundwater flux from the orientation of transmissivity (via the orientation of hydraulic conductivity interpolation function) model sensitivity tests.

Head Response to Orientation of Transmissivity					
Orientation:		0°	90°	180°	270°
Difference from 0° (mm)	EPA 2	0.00	520.0	1140.0	780.0
	EPA 3	0.00	440.0	870.0	570.0
	EPA 7	0.00	510.0	950.0	610.0
Groundwater Flux Response to Orientation of Transmissivity					
Orientation:		0°	90°	180°	270°
Difference from 0° (mm/day):		0.00	0.00	-0.01	0.01

Table 12c: Summary of the ranges of groundwater flux to the wetland with different curve numbers.

	Urban	CN sensitivity
Flux (mm/day)	0.244*	0.243*
Difference	0.001*	

*Based on the average of the time series data

Chapter 7: Discussion of Results

7.1 Discussion of Each Scenario's Flux

In general, the shape of the flux data across the constant head boundaries follows the shape of the calculated well hydrographs of EPA 2 and EPA7. Flux reaches a maximum sometime in March of 2008 and a minimum sometime in August 2008, for both pre-development and post-development scenarios. This corresponds to the days where the heads are near the highest and lowest calculated heads in EPA 2 and EPA 7. Therefore, when heads are at the yearly high a short time before spring when the vegetation is still dormant, model calculated baseflow is highest. This result is an agreement with the seasonal recharge observed in well hydrograph data at the field site.

On average, the relative difference in flux between urban and rural scenarios indicates a decrease in flux by 1.5%. The largest difference in flux occurred in March of 2008 (3.3%), which corresponds to the day when the watertable was close to its highest during the simulation. The decrease in calculated flux to the wetland in the urban scenario is consistent to what Erickson and Stefan (2009) and Rose and Peters (2001) report. However, the magnitude is not consistent. The relative difference in calculated flux to the wetland in the rural and urban scenarios should have increased as the simulation progressed and the calculated flux on the 423rd day of the simulation should have been near the difference that Rose and Peters (25% to 30%) or Erickson and Stefan report (30% to 40%) report. The anomalous model result is caused by the initial condition used in the simulation, which was based on steady-state conditions, or conditions that were representative of long term average conditions (see Table 9 in section 6.1

for a comparison of rainfall conditions during the simulation period and the long term average rainfall conditions). But the time period simulated was during a drought. This caused the simulated flux for both scenarios to be elevated, as the model was responding to the abnormally high (for the conditions) watertable. Because the excess drainage occurred in both scenarios, the difference between the scenarios was low.

The simulation was repeated using the end of the previous simulation as the initial condition for the new run. The relative difference between the calculated flux in the urban and rural scenario on the 423rd was 49%, which, agrees with Rose and Peters (2001) and Erickson and Stefan (2009). Figure 35 displays the calculated flux for each scenario and Table 13 displays the water budget results for each scenario simulated with the lower initial conditions.

On average the relative difference in flux to the wetland between the rural and leaky urban scenarios indicate an increase in flux by 13.2%. Once again, the relative difference was too low because the initial watertable conditions were too high which caused excess drainage in the rural scenario as the model responded to the very high watertable.

The leaky urban and rural scenario simulations were repeated using the end of the previous simulations as the initial conditions for the new run. The average relative difference was 80%. This indicates that the steady, daily recharge supplied by leaky utilities can supply enough additional recharge water to exceed baseflow in a rural scenario. Furthermore, leaky utilities may also provide sufficient water to maintain baseflow levels in times of drought.

A comparison of the flux calculated in the urban and leaky urban scenarios using the lower initial conditions indicates an increase in flux of 85%. This result indicates that this methodology has applications in identifying leaky utilities, as long as the utility is contributing a

significant amount of water to recharge (~100% of natural groundwater recharge in the urbanized scenarios).

On average, the relative difference in flux to the wetland between the rural and septic scenarios indicates an increase in flux by 27.0%. The increase is consistent with the work of Landers and Ankcorn (2008), while the magnitude of the increase is not. They find that during low flow periods caused by droughts that baseflow is, on average, 100% higher in areas with a high density of septic tanks. Again, the anomalous model result is caused by the initial condition used in the simulation, which was based on steady-state, or normal conditions. The initial conditions were too high for the drought conditions simulated which caused the simulated flux for the rural scenario to be elevated, because the model was responding to an abnormally high (for the conditions simulated) watertable. Because excess drainage occurred in rural scenario, the difference in flux between the rural and the septic scenarios was low.

The simulation was repeated using the end of the previous simulation as the initial condition for the new run. The relative difference between the calculated flux in the rural and septic scenario on the 423rd was 81%. This simulation showed that septic tanks can augment decreased natural recharge enough to exceed baseflow in rural watersheds.

The average relative percent difference in flux to the wetland between the rural and septic well scenario is 1.4%. Once again, the very low difference was caused by the high initial conditions.

The simulations were rerun with the initial conditions from the previous run of the rural scenario simulation. On average, the groundwater flux to the wetland in the septic well scenario was 76% higher than in the rural scenario. The continuous daily recharge supplied by the onsite wastewater disposal systems (OSWWDS) causes a constant relative increase in flux to the

wetland which indicates that the recharge in an urban scenario where houses are on OSWWDS and withdrawing water from the aquifer can still augment reduced natural recharge enough to exceed baseflow in rural scenarios as well. Figure 35 displays the calculated flux for each and Table 13 displays the water budget results for each scenario simulated with the lower initial conditions.

In conclusion, the results of the model simulations are consistent with the results of comparative studies and modeling studies in the literature. However, the model results are very sensitive to the initial conditions because the length of time of the conditions simulated is short (423 days). Care should be taken so that the data collected to calibrate the model is representative of the long term averages, or, that the initial conditions are representative of the hydraulic conditions simulated. Otherwise, the model results may be interpreted incorrectly.

7.2 Calculated Advective Velocities

The shape of the plot of calculated Darcy velocities in Figure 26 is similar to the shape of calculated heads in Figure 20 and Figure 21. The highest and lowest calculated advective velocities are near times when the head at wells EPA 2 and EPA 7 are the highest and lowest (late March and early January respectively). The maximum calculated advective velocity is 0.42 m/d. The advective velocity inferred by Amirithajah *et al.* (2002), which was 0.65 m/d. The difference in model calculated advective velocity and the inferred advective velocity indicates that a fast path was taken by the tracer through the vadose zone and the saprolite in the saturated zone. A comparison of model calculated advective velocity and the inferred advective velocity reported by Amirtharajah *et al.* (2002) show that their tracer utilized a fast path through a series of interconnected macropores, such as from a decayed root. Flow paths exist in the watershed that transmit water more rapidly than can be modeled because the flow paths followed by the

beads were on the very high end of the distribution of pore sizes. The model uses the average pore size distribution reflected in S_y and K, and thus cannot predict such an eventuality.

7.3 Discussion of the Sensitivity Analysis Results

The sensitivity analysis showed that the most influential factor in calculated head was recharge. Model calculated head showed moderate sensitivity to transmissivity with respect to the orientation of the hydraulic conductivity function and incremental changes, and to incremental changes specific yield. PET showed to have the least influence on model calculated head.

The sensitivity analysis also showed that orientation of transmissivity (via the orientation of the K interpolation function) and incremental changes in transmissivity along with recharge were the most influential parameters on calculated flux. Model calculated flux showed moderate sensitivity to incremental changes in specific yield. Incremental changes in PET showed to have the least influence on calculated flux.

Finally, the sensitivity analysis also showed that model calculated flux in a hypothesized urban setting was fairly insensitive to the choice of curve numbers for each scenario, as long as the range of the difference in the curve number assigned to the rural and urbanized scenario was 10 or less. The results of the sensitivity analysis are summarized in Tables 12a through 12c.

These results provide useful information for determining data collection and parameter estimation requirements. Data collection activities should focus on acquiring information about hydrologic factors that are poorly defined but have a great deal of influence on the groundwater system and the hypothesized urban settings to increase the accuracy of the model.

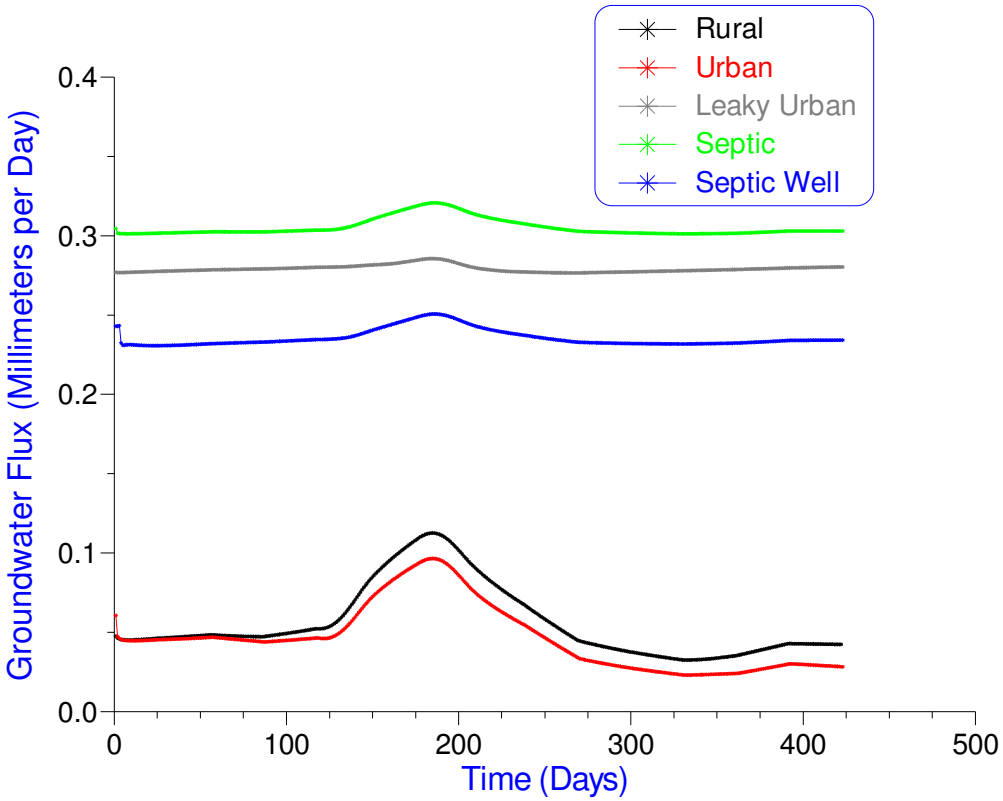

Figure 35: Groundwater flux to the wetland for each scenario using lower initial conditions.

Table 13: Water budget for each scenario simulation with lower initial conditions. . The values for each component of the budget are averages for the 423 day simulation. The value of each component is presented in terms of Flux (mm^3)/watershed area (mm^2). The superscripts denote the area over which a volume of water was applied, or the baseflow contributing area.

Scenario	Recharge[a] (mm/day)	PET[b] (mm/day)	Q_{septic}[c] (mm/day)	Q_{wells}[a] (mm/day)	$Q_{sewer/water}$[c] (mm/day)	$Q_{wetland}$[a] (mm/day)
Rural	0.12	2.58	0.00	0.00	0.00	0.06
Urban	0.08	2.58	0.00	0.00	0.00	0.05
Leaky Urban	0.08	2.58	0.00	0.00	11.00	0.28
Septic	0.08	2.58	450.00	0.00	0.00	0.31
Septic-well	0.08	2.58	450.00	-0.13	0.00	0.24

[a]Watershed area: 1.58E5 m^2

[b]Wetland torus area: 1091.65 m^2

[c]Leaky water/sewer pipes or septic leach field area: 25.28 m^2

Chapter 8: Conclusions

This work applies a method for evaluating the groundwater response to reduced natural recharge due to increased percent impervious surface that accompanies urbanization, recharge from leaky utilities and onsite waste water disposal systems, and withdrawal from the aquifer by single home wells. A finite element numerical model in planimetric view was calibrated for steady-state and transient conditions for the period of September 10, 2007 to November 3, 2008.

Five scenarios were simulated, one rural and four urbanized. Groundwater flux to a wetland was computed during each scenario simulation. A sensitivity analysis was performed to determine the impact of uncertainty among model parameters.

The model results showed that there was very little decline in discharge to the wetland between the rural and urbanized scenarios. The rural and urban scenario baseflow differed by 1.5% on average in the worst case of urbanization scenarios, where natural recharge is reduced due to increased percent impervious surface without additions from imported waters from leaky water mains and onsite wastewater disposal systems, when compared to computed groundwater flux for the natural system. This decline in baseflow is in agreement with the results in a similar study by Erickson and Stefan (2009) and Rose and Peters (2001), although the magnitude of the model computed baseflow decline results stand in contrast to the magnitude of the results of Rose and Peters (2001). The difference in magnitude can be attributed to the initial conditions used in the model being too high for the conditions simulated which elevated the groundwater flux to the wetland in the rural scenario and caused the relative differences between the rural and urbanized scenarios to be too low.

Relative difference in flux to the wetland increased, however, as the volume of imported water that becomes recharge increases, although, the relative percent difference among the fluxes computed for each scenario were very low compared to values taken from the literature. Once again, the difference in magnitude can be attributed to the model's initial conditions being too high for the conditions simulated which elevated the groundwater flux to the wetland in the rural scenario and caused the relative differences between the rural and urbanized scenarios to be low.

Regardless, after repeating each scenario simulation using the end of the previous simulation as the initial conditions for the new simulation, the relative differences between the rural scenario and the urban and septic scenarios are similar to the differences in baseflow reported in Rose and Peters (2001), Erickson and Stefan(2009), and Landers and Anckorn (2008). Additionally, the comparison of the leaky urban and urban scenarios indicates that this methodology has applications to identifying whether utilities are leaking or not, as long as the recharge supplied by the leaky utility is at least 100% of the natural groundwater recharge.

Because the initial conditions have a great deal of influence on the flux results in a simulation of this length of time, care should be taken to ensure that: (1) The data used to calibrate the model is representative of long term average conditions; or, (2) that the initial conditions are representative of the hydrologic conditions simulated.

A comparison of model calculated advective velocity and the inferred advective velocity reported by Amirtharajah *et al.* (2002) show that their tracer utilized a fast path through a series of interconnected macropores, such as from a decayed root. Therefore, flow paths exist on the watershed that are faster than the model can predict.

While this approach can be adapted and used by planners for site assessment of housing developments, the approach taken in this work was instrument, material, and time intensive

which limit its applicability as a planning tool to areas where groundwater records exist for some amount of time. Furthermore, this approach is limited by the limitations applicable to the curve number method outlined in TR-55 and TR-20.

The author makes five recommendations for future work: 1) Continue further head data collection at wells EPA 2 and EPA 7 so that the site can be modeled again for a much longer period of time to see how the response in calculated baseflow evolves over time; 2) investigate an urbanized site similar to the North Unit to obtain data on recharge and watertable behavior; 3) model the entire ARS North Unit (see Figure 3, page 10) and apply this methodology to test its applicability to larger watersheds; 4) continue work on this model to explore its applicability to water quality predictions for groundwater in different land use scenarios; and 5) continue testing the application of this methodology to identifying leaky water utilities.

References Cited

Allen R, Pereira L, Raes D, Smith M. 1998. *Crop Evapotranspiration: Guidelines for Computing Crop Water Requirements* Food and Agriculture Orginization of the United Nations (FAO) Rome.

Amirtharajah A, Young M, Pennell K, Steiner J, Fisher D, Endale D. 2002. Field transport of a Cryptosporidium surrogate in small catchments used for grazing lands In *Am. Water Works Assoc. Res. Foundation, Report*.

Anderson MP, Woessner WW. 1992. *Applied groundwater modeling: simulation of flow and advective transport*. Academic Press, Inc.: San Diego; 381.

Anonymous. Partners in Flight. http://www.blm.gov/wildlife/pl_11sum.htm accessed on July, 6 2010.

Anonymous.2002-2006. January 1, 2009. USGS Surface-Water Daily Data for Georgia http://nwis.waterdata.usgs.gov/ga/nwis/dv/?site_no=02221525&agency_cd=USGS&referred_module=sw.

Anonymous. National Oceanic and Atmospheric Administration. http://cdo.ncdc.noaa.gov/pls/plclimprod/poemain.cdobystn?dataset=DS3240&StnList=090435 accessed on January 1 2009.

Anonymous. U.S. Census Bureau. http://quickfacts.census.gov/qfd/states/13000.html accessed on April 12 2010.

Brassington FC, Rushton KR. 1987. A rising watertable in central Liverpool. *Quarterly Journal of Engineering Geology* **20**: 151-158.

Brooks RH, Corey AT. 1964. Hydraulic Properties of Porous Media In *Hydrology Paper,* Corey AT, Professor, Agricultural Engineering Department , Dils RE, Professor, College of Forestry and Range Management, Yevdjevich YM, Professor, Civil Engineering Department eds). Colorado State University: Fort Collins, Colorado;29pp.

Champion TM. 1989. Definition of hydrogeologic properties of soil and crystalline rock to determine the nature and extent of contamination at a site in the South Carolina Piedmont. In *Ground Water in the Piedmont*
III CD, White R, Stone P eds). Clemson Univsersity
46-55.

Cooper HH, Jacob CE. 1946. A generalized graphical method for evaluating formation constants and summarizing well field history. *American Geophysical Union Transactions* **v. 27**: pp. 526-534.

Courant R, Hilbert D. 1989. *Methods of mathematical physics.* . Interscience Publishers: New York; 856pp.

Cronshey R. 1975. *Urban hydrology for small watersheds*. U.S. Dept. of Agriculture, Soil Conservation Service, Engineering Division: Washington D.C.

Daniel CC, Dahlen PR. 2002. *Preliminary hydrogeologic assessment and study plan for a regional ground-water resource investigation of the Blue Ridge and Piedmont provinces of North Carolina*. US Dept. of the Interior, US Geological Survey.

Dunne T, Leopold LB. 1978. *Water in Environmental Planning*. WH Freeman: San Franscisco; 818.

Endale DM, Fisher DS, Steiner JL. 2006. Hydrology of a zero-order Southern Piedmont watershed through 45 years of changing agricultural land use. Part 1. Monthly and seasonal rainfall-runoff relationships. *Journal of Hydrology* **316**: 1-12.

Erickson TO, Stefan HG. 2009. Natural Groundwater Recharge Response to Urbanization: Vermillion River Watershed, Minnesota. *Journal of Water Resources Planning and Management* **135**: 512-520.

Fanning JL. 2003. Water use in Georgia by county for 2000 and water-use trends for 1980-2000. Survey GGSiCwUSG. Atlanta, GA Information Circular 106

FAO. 1998. World reference base for soil resources. In *World Soil Resources Reports No. 84*. Rome.

Fennessey LAJ, Miller AC, Hamlett JM. 2001. Accuracy and precision of NRCS models for small watersheds. *Journal of the American Water Resources Association* **37**: 899-912.

Flight Pi. http://www.blm.gov/wildlife/pl_11sum.htm accessed on July, 6 2010.

Foster SSD. 1988. Impacts of urbanization on groundwater In *Hydrological processes and water management in urban areas,* Massing H ed. IAHS;187-207.

Franzluebbers AJ, Schomberg HH, Endale DM. 2007. Surface-soil responses to paraplowing of long-term no-tillage cropland in the Southern Piedmont USA. *Soil & Tillage Research* **96**: 303-315.

Freeze R, Cherry J. 1979. *Groundwater*. Prentice-Hall Englewood Cliffs, NJ; 604.

Freeze RA, Witherspoon PA. 1967. Theoretical analysis of regional groundwater flow. 2. Effect of water-table configuration and subsurface permeability variation. *Water Resources Research* **3**: 623-634.

Green WH, Ampt GA. 1911. Studies on soil physics, I. The flow of air and water through soils. *Journal of Agricultural Science* **4**: 1-24.

Hack J. 1989. Geomorphology of the Appalachian highlands In *The Appalachian-Ouachita Orogen in the United States. The Geology of North America* Hatcher RD, Thomas WA, Viele GW eds). Geological Society of America: Boulder, CO;459-470.

Healy RW, Cook PG. 2002. Using groundwater levels to estimate recharge. *Hydrogeology Journal* **10**: 91-109.

Hershfield DM. 1961. *Rainfall frequency atlas of the United States : for durations from 30 minutes to 24 hours and return periods from 1 to 100 years*. Dept. of Commerce, Weather Bureau: Washington D.C.

Hoogenboom G. http://www.griffin.uga.edu/aemn/cgi-bin/AEMN.pl?site=GAWH&report=hi accessed on January 1 2009.

Kalaidzidou-Paikou N, Karamouzis D. 1995. Unsteady groundwater flow over sloping beds In *Water Resources Management Under Drought or Water Shortage Conditions*. Balkema A.A.: Nicosia, Cyprus;127-133.

Kent WM. 1973. A Method for Estimating Volume and Rate of Runoff in Small Watersheds In *Technical Paper 49*. U.S. Department of Agriculture Soil Conservation Service (SCS): Washington, DC.

Ku HFH, Hagelin NW, Buxton HT. 1992. Effects of urban storm-runoff control on ground-water recharge in Nassau County, New York. *Ground Water* **30**: 507-514.

Landers MN, Ankcorn PD. 2008. Methods to evaluate influence of onsite septic wastewater-treatment systems on base flow in selected watersheds in Gwinnett County, Georgia, October 2007 Survey USG ed.;12.

Landers MN, Ankcorn PD, McFadden KW. 2007. Watershed effects on streamflow quantity and quality in six watersheds of Gwinnett County, Georgia. USGS. 2007-5132

LeGrand H. 2004. A master conceptual model for hydrogeological site characterization in the piedmont and mountain region of North Carolina: a guidance manual. *North Carolina Department of Environment and Natural Resources, Raleigh, NC*.

LeGrand HE. 1989. A conceptual model of ground water settings in the Piedmont region In *Ground Water in the Piedmont,* Daniel C, White R, Stone P (eds). Clemson University;317-327.

LeGrand HE. 2004. A master conceptual model for hydrogeological site characterization in the Piedmont and Mountain region of North Carolina: A guidance manual. North Carolina Department of Environmental and Natural Resources: 55

Leonard RA, Langdale GW, Fleming WG. 1979. Herbicide Runoff from Upland Piedmont Watersheds Data and Implications for Modeling Pesticide Transport. *Journal of Environmental Quality* **8**: 223-229.

Lerner DN. 1986. Leaking pipes recharge groundwater. *Ground Water* **24**: 654-662.

Lerner DN. 2002. Identifying and quantifying urban recharge: a review. *Hydrogeology Journal* **10**: 143-152.

McCuen RH. 2005. *Hyrdrologic Analysis and Design*. Pearson Prentic Hall; 859.

McFarland RE. 1989. Ground-Water hydrology, geochemistry, and nitrogen transport in a saprolite-fractured schist aquifer under agricultrual land in the piedmont physiographic province of Maryland In *GROUNDWATER in the PIEDMONT* Charles C. Daniel I, White RK, Stone PA (eds). Clemson Univsersity 442-454.

Nelson AB. 1989. Hydraulic relationship between a fractured bedrock aquifer and a primary stream, North Carolina Piedmont In *GROUNDWATER in the PIEDMONT*. Clemson University;159-162.

Overbaugh M. 1996. Survey of the Physical Properties of Saprolite. *Department of Geology*. University of Georgia: Athens.

Perkins HF. 1987. *Characterization Data for Selected Georgia Soils*. Georgia Agricultural Experiment Stations, College of Agriculture, University of Georgia.

Price M, Reed DW. 1989. THE INFLUENCE OF MAINS LEAKAGE AND URBAN DRAINAGE ON GROUNDWATER LEVELS BENEATH CONURBATIONS IN THE UK. *Proceedings of the Institution of Civil Engineers Part 1-Design and Construction* **86**: 1019-1020.

Railsback LB, Bouker PA, Feeney TP, Goddard EA, Hall AS, Jackson BP, McClain AA, Orsega MC, Rafter MA, Webster JW. 1996. A survey of the major-element geochemistry of Georgia groundwater. *Southeastern Geol* **36**: 99–122.

Rankin B. Atlanta Journal Constitution. http://www.ajc.com/news/federal-judge-rules-against-94051.html accessed on April 12 2010.

Reynolds RJ. 1982. Base flow of streams on Long Island, New York. 81-48

Robertson SM. 1968. Soil Survey of Clarke and Oconee Counties, Georgia. *USDA Soil Conservation Service in Cooperation with Univ. Georgia, Coll. Agric., Agric. Expt. Stations. US Govt. Printing Off., Washington, DC*.

Rose S, Peters NE. 2001. Effects of urbanization on streamflow in the Atlanta area(Georgia, USA): a comparative hydrological approach. *Hydrological Processes* **15**: 1441-1457.

S.C.S. 1965. *Computer program for project formulation : hydrology*. Dept. of Agriculture, Soil Conservation Service, Engineering Division, Central Technical Unit: Washington.

Scanlon BR, Healy RW, Cook PG. 2002. Choosing appropriate techniques for quantifying groundwater recharge. *Hydrogeology Journal* **10**: 18-39.

Schumak BBG, Neil J.; Smith, Jimmy N. 1989. Fracture trace analysies and other investigative techniques for determination of conductive zones in rock at a chemical manufacturing facility in the piedmont In *Proceedings of a Conference on GROUND WATER in the PIEDMONT of the Eastern United States,* Charles C. Daniel I, Richard K White, Peter A. Stone ed.: Clemson, S.C., Clemson Univsersity;349-358.

Shaw E. 1994. *Hydrology in practice*. Chapman & Hall: London.

Sloto RA, Crouse MY. 1996. HYSEP: A computer program for streamflow hydrograph separation and analysis In *United States Geological Survey Water-Resources Investigation Report*.46.

Sophocleus M. 2002. Interactions between groundwater and surface water: The state of the science. *Hydrogeology Journal* **10**: 52-67.

Thornthwaite C. 1948. An approach toward a rational classification of climate. *Geographical review* **38**: 55-94.

Toth J. 1962. A Theory of Groundwater Motion in Small Drainage Basins in Central Alberta, Canada. *Journal of Geophysical Research* **67**: 4375-4387.

Toth J. 1963. A Theoretical Analysis of Groundwater Flow in Small Drainage Basins. *Journal of Geophysical Research* **68**: 4795-4812.

Washington JW, Endale DM, Samarkina LP, Chappell KE. 2004. Kinetic control of oxidation state at thermodynamically buffered potentials in subsurface waters. *Geochimica et Cosmochimica Acta* **68**: 4831-4842.

Washington JW, Thomas RC, Endale DM, Schroer KL, Samarkina LP. 2006. Groundwater N speciation and redox control of organic N mineralization by O 2 reduction to H 2 O 2. *Geochimica et cosmochimica acta* **70**: 3533-3548.

West LT, Abreu MA, Bishop JP. 2008. Saturated hydraulic conductivity of soils in the Southern Piedmont of Georgia, USA: Field evaluation and relation to horizon and landscape properties. *Catena* **73**: 174-179.

Yang Y, Lerner DN, Barrett MH, Tellam JH. 1999. Quantification of groundwater recharge in the city of Nottingham, UK. *Environmental geology* **38**: 183-198.